ABSTRACT

QUADRANT PLATE PROPORTIONAL WEIRS

Nguyen van Tao

Linear proportional weirs find many diverse engineering applications such as flow-measuring devices and outlets for sediment chambers. Available exact solutions to generate the weir profiles characterised by a linear head-discharge relationship involve considerable mathematical complexities. Recent studies have indicated that simple weir shapes formed of two quadrants attached to rectangular bases possessed linear head-discharge relationships. In the present study, the characteristics of flow through quadrant plate weirs having triangular and circular bases are obtained theoretically. Functional relationships between the coefficient of discharge and the other characteristic weir flow parameters are established. Experimental studies were conducted on selected weirs and the test results are in agreement with the theoretical predictions. Based on the present study, it is established that the coefficient of discharge C_d is nearly constant for the quadrant plate weir when the weir parameter P/R exceeds 0.5. Design charts have been prepared for the quadrant plate weirs which have rectangular, triangular and circular bases.

ACKNOWLEDGEMENTS

ACKNOWLEDGEMENTS

The author wishes to thank Dr. A.S. Ramamurthy and Dr. B.S. Pani for suggesting this topic.

The assistance of Mr. Louis Stankevicius and Mr. Daniel Roy of the Water Resources Laboratory in the fabrication of equipment is thankfully acknowledged.

TABLE OF CONTENTS

TABLE OF CONTENTS

LIST OF TABLES

LIST OF TABLES

LIST OF FIGURES

LIST OF FIGURES

LIST OF NOTATIONS

LIST OF NOTATIONS

a	Height of the weir base
b	top width of the weir
C_d	coefficient of discharge of quadrant plate proportional weir
F	Froude number
g	gravitational acceleration
H	head acting over the datum
H'	head acting over the crest
K	dimensional constant of proportionality
m	index
P	height of the crest above the channel bed level
Q	theoretical discharge through the quadrant plate proportional weir
Q_1	theoretical discharge through the rectangular base weir
Q_1'	theoretical discharge through the triangular base weir
Q_1''	theoretical discharge through the circular base weir
Q_2	theoretical discharge through the rectangular weir enveloping the quadrants
Q_3	theoretical discharge through the two quadrants
Q_{ac}	actual discharge through the quadrant plate proportional weir
Q_0	actual full discharge through the quadrant plate proportional weir
Q_{non}	non-dimensional form of discharge

$$Q_{non} = \frac{Q}{[2(2g)^{1/2}R^{5/2}]} = \frac{Q_{ac}}{[2C_d(2g)^{1/2}R^{5/2}]}$$

R	radius of the quadrant edge weir
R_0	radius of the circular base weir
V	mean velocity in the approach channel
x	half-width of incremental area as defined in Fig. 2(d)
x'	half-width of incremental area as defined in Fig. 3(b)
x''	half-width of incremental area as defined in Fig. 4(b)
y	height of incremental area above the crest
w	base width of the weir
α	intermediate angle as defined in Fig. 2(d)
β	intermediate angle as defined in Fig. 3(b)
γ	intermediate angle as defined in Fig. 4(b)
λ	factor of reduction of head for the location of head datum
Γ	gamma function
η_a	ratio of weir base height a to radius R of quadrant
η_b	ratio of top width b of the weir to radius R of quadrant
η_H	ratio of head H acting over the crest to radius R of quadrant
η_{R_0}	ratio of radius R_0 of the circular base to radius R of quadrant
η_y	ratio of incremental area height y to radius of quadrant

CHAPTER I

INTRODUCTION

CHAPTER I

INTRODUCTION

A weir is a structure built across a river or a channel in order to raise the level of water and to divert it. The depression in the side of a tank, a reservoir or a channel for passing surplus water, an overflow structure associated with a dam, or other similar overflow structures are also referred to as weirs [3]. A proportional weir is a weir with a profile such that the discharge is a desired function of the head causing flow. Brenke used Abel's integral equations to obtain the profiles of certain proportional weirs [3]. Cowgill followed the same procedure as Brenke [3] to achieve the discharge-head relation given by

$$Q = Kh^m \tag{1.1}$$

He obtained an equation for the weir profile given by

$$x(y) = \frac{2K\Gamma(m+1)y^{m-3/2}}{\pi^{1/2}\Gamma(m-\frac{1}{2})} \tag{1.2}$$

where

Q = discharge passing through the weir

K = dimensional constant of proportionality

h = head over the crest of the weir

m = index

x(y) = half-width of the weir at any height y

Γ = familiar Gamma function

Examining the above equation we note that $x \to \infty$ as $y \to 0$ when $m < \frac{3}{2}$. It is, therefore, impracticable to construct a weir of infinite width. In order to overcome the practical limitations of the infinite width, the infinite bottom wings of the weir were cut off and replaced by the circular openings. However, this method seems to be approximate. The exact method is to provide a base weir and to account for it while designing the proportional weir, but the head has to be measured from a certain datum [3]. Since the discharge of such a weir is proportional to the first power of the head on the weir (m=1), the name Linear Proportional Weir is given to it.

Linear proportional weirs find many diverse engineering applications such as flow measuring devices, outlets for sediment chambers, controls for float regulated dosing and chemical sampling. The profile of a linear proportional weir depends on the shape of the base weir which may be parabolic, triangular, trapezoidal, circular or rectangular. In order to simplify the construction of linear proportional weirs, a quadrant plate weir was designed involving two quadrants of circles with rectangular bases [2]. The portion of the weir profile exclusive of the base weir is termed the proportional portion. The linearity of the discharge-head relation holds for the entire weir after the flow depth enters the proportional portion. The discharge that flows through the base weir before the flow enters the proportional portion may be considered waste since it would not be governed by the proportionality relation.

In the present study, a similar approach has been extended to quadrant plate weirs which have triangular and circular base weirs (Figure 1). Numerical integration techniques were applied to obtain the theoretical head-discharge relationship for linear proportional weirs assuming the invariance of the weir discharge coefficient, C_d. Design charts have been prepared for a quick solution to a given set of parameters that characterise the weir flow. In the ensuing discussion, linear weirs denote weirs for which the head discharge relationship is linear.

CHAPTER II

THEORETICAL CONSIDERATIONS

CHAPTER II

THEORETICAL CONSIDERATIONS

Since the head causing flow through the weir has to be measured from a certain datum, the general discharge equation may be considered to be of the following form [1,4,5]

$$Q = K(H-\lambda a) \tag{2.1}$$

where

$\lambda = \frac{1}{3}$ for rectangular base weirs

$\lambda = \frac{3}{5}$ for triangular base weirs

or

$$Q = K(H-\lambda R) \tag{2.2}$$

where

$\lambda = \frac{1}{2}$ for circular base weirs

In the above equations, the value of K is not known a priori, since the discharge coefficient C_d has to be determined experimentally. The exact solutions assume that the value of C_d is constant. Consequently, the tested weirs based on these solutions are expected to possess only approximate head-discharge relationships. The principal parameters that govern the head discharge relationship are given in the non-dimensional form

$$Q_{non} = \frac{Q_{ac}}{[2\, C_d (2g)^{1/2} R^{5/2}]} \tag{2.3}$$

where

Q_{non} = non-dimensional form of discharge and its values are calculated by numerical integration techniques

Q_{ac} = actual discharge measured experimentally

Knowing Q_{non} and Q_{ac}, one can calculate C_d.

2.1 RECTANGULAR BASE WEIR

The flow through the quadrant plate weir can be viewed as the flow through different sections of the weir, as shown in Fig. 2(a).

2.1.1 Computation of the theoretical discharge Q_1 through the rectangular base weir

For the flow configuration shown in Figure 2(b),

$$V = [2g(H-y)]^{1/2}.$$

and

$$dq = (b+2R)\,dy\,[2g(H-y)]^{1/2}$$

dividing both sides by $R^{5/2}$ to nondimensionalize the equations, one gets

$$\frac{dq}{R^{5/2}} = \left[\left(\frac{b+2R}{R}\right)\right]\left[2g\left(\frac{H-y}{R}\right)\right]^{1/2}\left(\frac{dy}{R}\right)$$

The following relation is obtained for the base weir flow when the above equation is integrated with respect to y. Thus,

$$\frac{Q_1}{R^{5/2}} = \left[\left(\frac{b+2R}{R}\right)\right](2g)^{1/2} \int_0^{a/R} \left[\left(\frac{H-y}{R}\right)\right]^{1/2} d\left(\frac{y}{R}\right)$$

$$(\eta_b+2)(2g)^{1/2} \int_0^{\eta_a} (\eta_H-\eta_y)^{1/2}\, d\eta_y$$

$$= (\eta_b+2)(2g)^{1/2}\left[\left(\frac{2}{3}\right)\left(\frac{\eta_H-\eta_y}{-1}\right)^{3/2}\right]_0^{\eta_a}$$

$$= (\eta_b+2)(2g)^{1/2} 2[\eta_H^{3/2} - (\eta_H-\eta_a)^{3/2}]$$

Or,

$$\frac{Q_1}{[2(2g)^{1/2}R^{5/2}]} = \left[\left(\frac{\eta_b+2}{3}\right)\right][\eta_H^{3/2} - (\eta_H-\eta_a)^{3/2}] \qquad (2.4)$$

2.1.2 Computation of the theoretical discharge Q_2 through the rectangular weir enveloping the quadrants

For the flow configuration shown in Figure 2(c)

$$V = [2g(H-y)]^{1/2}$$

and

$$dq = (b+2R)\,dy\,[2g(H-y)]^{1/2}$$

dividing both sides by $R^{5/2}$ to non-dimensionalize the equation, one gets

$$\frac{dq}{R^{5/2}} = \left[\left(\frac{b+2R}{R}\right)\right]\left[2g\left(\frac{H-y}{R}\right)\right]^{1/2} \left(\frac{dy}{R}\right)$$

The following relation is obtained for the top weir flow (including the flow through two quadrants) when the above equation is integrated with respect to y. Thus

$$\frac{Q_2}{R^{5/2}} = \left[\left(\frac{b+2R}{R}\right)\right] (2g)^{1/2} \int_{a/R}^{H/R} \left[\left(\frac{H-y}{R}\right)\right]^{1/2} d\left(\frac{y}{R}\right)$$

$$= (\eta_b+2)(2g)^{1/2} \int_{\eta_a}^{\eta_H} (\eta_H-\eta_y)^{1/2} d\eta_y$$

$$= (\eta_b+2)(2g)^{1/2} \left[\left(\frac{2}{3}\right)\left(\frac{\eta_H-\eta_y}{-1}\right)^{3/2}\right]_{\eta_a}^{\eta_H}$$

$$= (\eta_b+2)(2g)^{1/2} \left(\frac{2}{3}\right)(\eta_H-\eta_a)^{3/2}$$

Or

$$\frac{Q_2}{[2(2g)^{1/2}R^{5/2}]} = \left[\left(\frac{\eta_b+2}{3}\right)\right][(\eta_H-\eta_a)^{3/2}] \qquad (2.5)$$

2.1.3 Computation of the theoretical discharge Q_3 through the two quadrants

The weir flow through the two quadrant can be considered as the weir flow through the half-circle having a radius of R.

$$V = [2g(H-y)]^{1/2}$$

$$x = R \sin\alpha$$

$$\cos\alpha = \left(\frac{a+R-y}{R}\right)$$

$$x = [(a+2R-y)(y-a)]^{1/2}$$

and

$$dq = 2[(a+2R-y)(y-a)]^{1/2}\, dy[2g(H-y)]^{1/2}$$

dividing both sides by $R^{5/2}$ to nondimensionalize the equations, one gets

$$\frac{dq}{R^{5/2}} = 2\{[(\frac{a+2R-y}{R})][(\frac{y-a}{R})]\}^{1/2}\ (\frac{dy}{R})[2g(\frac{H-y}{R})]$$

$$= 2[(\eta_a-\eta_y+2)(\eta_y-\eta_a)]^{1/2}(2g)^{1/2}[(\eta_H-\eta_y)]^{1/2}\, d\eta_y$$

The following relation is obtained for the weir flow through two quadrants when the above equation is integrated with respect to y.

Thus,

$$\frac{Q_3}{[2(2g)^{1/2}R^{5/2}]} = \int_{\eta_a}^{\eta_H} [(\eta_a-\eta_y+2)(\eta_y-\eta_a)(\eta_H-\eta_y)]^{1/2}\, d\eta_y \quad (2.6)$$

The total weir flow through the quadrant plate proportional weir is therefore obtained by deducting Q_3 from the sum of Q_1 and Q_2.

$$Q = Q_1 + Q_2 - Q_3 .$$

$$\frac{Q}{[2(2g)^{1/2}R^{5/2}]} = [(\frac{\eta_b+2}{3})][\eta_H^{3/2} - (\eta_H-\eta_a)^{3/2}]$$

$$+ [(\frac{\eta_b+2}{3})][(\eta_H-\eta_a)^{3/2}]$$

$$- \int_{\eta_a}^{\eta_H} [(\eta_a-\eta_y+2)(\eta_y-\eta_a)(\eta_H-\eta_y)]^{1/2} d\eta_y$$

Rearranging and noting that $Q = \frac{Q_{ac}}{C_d}$, one gets

$$Q_{non} = \frac{Q_{ac}}{[2\ C_d(2g)^{1/2}\ R^{5/2}]}$$

$$= (\frac{\eta_b+2}{3})]\eta_H^{3/2} - \int_{\eta_a}^{\eta_H} [(\eta_a-\eta_y+2)(\eta_y-\eta_a)(\eta_H-\eta_y)]^{1/2} d\eta_y \qquad (2.7)$$

2.2 TRIANGULAR BASE WEIR

Following the same computation as above, the total weir flow through the quadrant plate proportional weir with triangular base weir is obtained by computing only the weir flow Q_1' through the triangular base weir. (Figure 3(a))

2.2.1 Computation of the theoretical discharge Q_1' through the triangular base weir

For the flow configuration shown in Figure 3(b)

$$V = [2g(H-y)]^{1/2}$$

$$\text{Tan}\beta = \frac{x'}{y} = (\frac{R+b/2}{a})$$

$$x' = \left(\frac{y}{a}\right)\left(R + \frac{b}{2}\right)$$

and

$$dq = \left(\frac{y}{a}\right)(2R + b)\, dy' \left[2g(H-y)\right]^{1/2}$$

dividing both sides by $R^{5/2}$ to nondimensionalize the equations, one gets

$$\frac{dq}{R^{5/2}} = \left(\frac{y}{a}\right)\left[\left(\frac{2R+b}{R}\right)\right]\left(\frac{dy}{R}\right)\left[2g\left(\frac{H-y}{R}\right)\right]^{1/2}$$

The following relation is obtained for the triangular base weir flow when the above equation is integrated with respect to y. Thus,

$$\frac{Q_1'}{R^{5/2}} = \left[\left(\frac{2R+b}{R}\right)\right](2g)^{1/2}\left(\frac{1}{a}\right)\int_0^{a/R}\left(\frac{y}{R}\right)\left[\left(\frac{H-y}{R}\right)\right]^{1/2} d\left(\frac{y}{R}\right)$$

$$= \left[\left(\frac{\eta_b+2}{\eta_a}\right)\right](2g)^{1/2}\int_0^{\eta_a} \eta_y(\eta_H-\eta_y)^{1/2}\, d\eta_y$$

Or

$$\frac{Q_1'}{\left[2(2g)^{1/2} R^{5/2}\right]} = \left[\left(\frac{\eta_b+2}{15\eta_a}\right)\right]\left[2\eta_H^{5/2} - (2\eta_H+3\eta_a)(\eta_H-\eta_a)^{3/2}\right] \tag{2.8}$$

The total weir flow through the quadrant plate proportional weir with triangular base weir is therefore obtained by deducting Q_3 from the sum of Q_1' and Q_2 (Fig. 3(c) and Fig. 3(d)).

Noting also that

$$Q = \frac{Q_{ac}}{C_d},$$

one gets

$$Q_{non} = \frac{Q_{ac}}{[2\ C_d (2g)^{1/2} R^{5/2}]}$$

$$= [(\frac{\eta_b+2}{15\eta_a})][2\eta_H^{5/2} - (2\eta_H+3\eta_a)(\eta_H-\eta_a)^{3/2}]$$

$$+ [(\frac{\eta_b+2}{3})][(\eta_H-\eta_a)^{3/2}]$$

$$- \int_{\eta_a}^{\eta_H} [(\eta_a-\eta_y+2)(\eta_y-\eta_a)(\eta_H-\eta_y)]^{1/2}\ d\eta_y \qquad (2.9)$$

2.3 CIRCULAR BASE WEIR

Similarly, the total weir flow through the quadrant plate proportional weir with circular base weir is treated as the flow through different sections of the weir as shown in Figure 4(a).

2.3.1 Computation of the theoretical discharge Q''_1 through the circular base weir

For the flow configuration, as shown in Figure 4(b)

$$V = [2g(H-y)]^{1/2}$$

$$x'' = R_0 \sin\gamma$$

$$\cos\gamma = (\frac{R_0-y}{R_0})$$

$$x'' = (2y\ R_0 - y^2)^{1/2}$$

and

$$dq = 2(2y\ R_0 - y^2)^{1/2}\ dy\ [2g(H-y)]^{1/2}$$

Dividing both sides by $R^{5/2}$ to nondimensionalize the equations, one gets

$$\frac{dq}{R^{5/2}} = 2\left[\left(\frac{2y\ R_0 - y^2}{R^2}\right)\right]^{1/2} \left(\frac{dy}{R}\right) \left[2g\left(\frac{H-y}{R}\right)\right]^{1/2}$$

The following relation is obtained for the circular base weir flow when the above equation is integrated with respect to y.

$$\frac{Q_1''}{R^{5/2}} = 2(2g)^{1/2} \int_0^{\eta_a} [\eta_y(2\eta_{R_0} - \eta_y)(\eta_H - \eta_y)]^{1/2}\ d\eta_y$$

or

$$\frac{Q_1''}{[2(2g)^{1/2}\ R^{5/2}]} = \int_0^{\eta_a} [\eta_y(2\eta_{R_0} - \eta_y)(\eta_H - \eta_y)]^{1/2}\ d\eta_y \qquad (2.10)$$

The total weir flow through the quadrant plate proportional weir with circular base weir is therefore obtained by deducting Q_3 from the sum of Q_1'' and Q_2 (Figures 4(c) and 4(d)).

Noting also that

$$Q = \frac{Q_{ac}}{C_d},$$

one gets

$$Q_{non} = \frac{Q_{ac}}{[2\ C_d(2g)^{1/2}\ R^{5/2}]}$$

$$= \int_0^{\eta_a} [\eta_y(2\eta_R - \eta_y)(\eta_H - \eta_y)]^{1/2}\, d\eta_y$$

$$+ [(\frac{\eta_b+2}{3})](\eta_H - \eta_a)^{3/2}$$

$$- \int_{\eta_a}^{\eta_H} [(\eta_a - \eta_y + 2)(\eta_y - \eta_a)(\eta_H - \eta_y)]^{1/2}\, d\eta_y \qquad (2.11)$$

Assuming C_d to be a constant, equations (2.7), (2.9) and (2.11), were solved numerically by using numerical integration techniques, in which $d\eta_y$ is incremented by 0.01, starting from the lower limit to the upper limit, and η_H is incremented by 0.1, starting from η_a to η_a+1. The numerical values of η_a and η_b are determined by trial and error, a different set of (η_a, η_b) are selected and the maximum theoretical deviation from linearity in percentage are calculated. Trial solutions obtained are shown in the following tables.

TABLE 2.1 TRIAL SOLUTIONS

Series	Base Type	η_a	η_b
1	Triangular	0.50	0.80
2	Triangular	0.35	0.65
3	Circular	0.374	0.90

TABLE 2.2 NUMERICAL VALUES OF EQUATION (2.9) WITH $\eta_a = 0.50$ AND $\eta_b = 0.80$ AND ITS DEVIATIONS. SERIES 1

H/R	Q_{non}	Q/Q_0	DEVIATION FROM LINEARITY (%)
0.5	.1320	.1584	0.000
0.6	.2008	.2411	-0.604
0.7	.2718	.3263	-0.143
0.8	.3434	.4122	0.323
0.9	.4149	.4981	0.609
1.0	.4860	.5834	0.715
1.1	.5564	.6679	0.679
1.2	.6261	.7516	0.547
1.3	.6953	.8347	0.364
1.4	.7642	.9174	0.169
1.5	.8331	1.0000	0.000

TABLE 2.3 NUMERICAL VALUES OF EQUATION (2.9) WITH $\eta_a = 0.35$ AND $\eta_b = 0.65$ AND ITS DEVIATIONS. SERIES 2

H/R	Q_{non}	Q/Q_0	DEVIATION FROM LINEARITY (%)
.35	.0731	.1125	0.000
.45	.1290	.1983	-1.460
.55	.1875	.2883	-0.590
.65	.2469	.3797	0.243
.75	.3063	.4710	0.760
.85	.3653	.5617	0.979
.95	.4236	.6513	0.970
1.05	.4811	.7397	0.807
1.15	.5379	.8271	0.554
1.25	.5942	.9137	0.268
1.35	.6504	1.0000	0.000

TABLE 2.4 NUMERICAL VALUES OF EQUATION (2.11) WITH $\eta_a = .374$, $\eta_b = 0.90$, $R_0 = 3R$ AND ITS DEVIATIONS. SERIES 3

H/R	Q_{non}	Q/Q_0	DEVIATION FROM LINEARITY (%)
.374	.1278	.1458	0.000
.474	.2024	.2308	-0.170
.574	.2772	.3161	-0.165
.674	.3527	.4023	0.067
.774	.4285	.4887	0.249
.874	.5040	.5748	0.331
.974	.5790	.6604	0.323
1.074	.6537	.7456	0.253
1.174	.7281	.8304	0.155
1.274	.8024	.9151	0.061
1.374	.8768	1.0000	0.000

CHAPTER III

EXPERIMENTAL SET-UP AND PROCEDURE

CHAPTER III

EXPERIMENTAL SET-UP AND PROCEDURE

The objective of the present experimental investigation was to verify the linear proportionality of Quadrant Plate Proportional Weir with triangular and circular base weir and to determine the value of C_d for further designs.

Quadrant edge weirs of the required dimensions were cut out of 6 mm thick plexiglas sheets. The thickness of all the edges was 1.25 mm and bevelled at 45°. The experimental set-up (Fig. 5) consists of a horizontal recirculating steel flume 40.6 cm wide and 3.05 m long. Suitable screens and an approach floor were provided to obtain a smooth and level flow surface near the section where the head causing the weir flow was measured.

Weir plates were fixed at the outlet end of the flume with the crests levelled at the desired height above the bed. The supply was provided through two 7.6 cm diameter pipes connected to a centrifugal pump. The discharge from the quadrant edge weir was led into another steel flume fitted with a 90° V-notch conforming to flow measuring standards. The head over the crest of the proportional weir and the V-notch were measured by precision point gauges which could read to the nearest 0.01 in.

Each of the series of weirs was tested by locating the weir at different crest heights, P, above the channel bed

level. P is the level difference between the crest level and the channel bed level. At the start of the experiment, the full discharge Q_o was allowed to pass through the proportional portion and this was reduced incrementally in order to record the discharge passing through at different heads. Considerable settling time was necessary to stabilise the weir discharge and ensure steady flow through the weir system before the readings could be taken. At the end of the tests, the inlet valves were shut off and the water level corresponding to the weir crest was recorded. A large waiting time was needed to record the weir crest level. In a typical series, the height P was set at 9.50 in, 5 in, 2.37 in, 1.11 in, 0.24 in (Serie 1).

CHAPTER IV

ANALYSIS OF RESULTS

CHAPTER IV

ANALYSIS OF RESULTS

4.1 EXPERIMENTAL DATA

The experimental results related to the variation of the actual discharge Q_{ac} through the Quadrant Plate Proportional Weirs with head H over the weir datum are given in Fig. 6. The trend of the H-Q_{ac} curve is linear and validates the theoretical predictions for the three series shown. Theoretically, the linear relationship is predicted when the head registered corresponds to the top of the weir base. However, as a consequence of the inherent draw down accompanying terminal flow, deviations from the linearity relationship is to be expected when the head registered is only slightly above the top of the base section. Columns (3) and (4) of Tables A.1, A.2,A.3 are set in the non-dimensional form by dividing the actual discharge Q_{ac} by the maximum discharge Q_o, the head H is divided by the radius R of the quadrant. The head-discharge relationship is also plotted in the non-dimensional form in Fig.7. Column (5) of Tables 2.2, 2.3 and 2.4 denotes Q_{non} and is derived from column (4). Knowing Q_{ac} and Q_{non}, column (6), C_d can be calculated by using Equation (2.3). Column (7) is the mean velocity V in the approach channel given by

$$V = \frac{Q_{ac}}{\text{Cross-sectional area of channel}}$$

$$V = \frac{Q_{ac}}{(H'+P)(40.6\ cm)(.397\ in/cm)/(144\ in^2/ft^2)}$$

$$V = \frac{Q_{ac}}{0.112(H'+P)} \qquad (4.1)$$

The Froude number F in column (8) is given by

$$F = \frac{V}{[g(H'+P)]^{\frac{1}{2}}} \qquad (4.2)$$

The variation of the discharge coefficient C_d with the non-dimensional form of head H/R is given in Figure 8, which shows that the coefficient of discharge C_d decreases with head H. In an earlier series of tests on Quadrant Plate Proportional Weirs with rectangular base weir [2] it was observed that the coefficient of discharge C_d exhibited a tendency to increase at low head, reaching a maximum value, and then decrease. Such a phenomenon was also observed in the present investigation, especially in the Serie 1, with a triangular base weir. The assumption of the invariance of C_d was ensured only for high P/R values. In fact, for the weirs tested, the value of C_d is highly variable for values of P/R which are below 0.5 (Fig. 9). Figure 9 is generated using Figure 8 to indicate the effect of P/R on C_d. For very large P/R values, C_d seems to approach asymtotically the value of 0.62 for all H/R. When P/R is below 0.5, the coefficient of discharge C_d varies in the limited range of 5% beyond 0.62. Low values of P/R also resulted in a higher range of Froude number.

For full flow conditions, C_d is a strong function of the Froude number F which reflects the effects of the velocity of approach [2]. Figure 10 indicates the location of the datum for the Quadrant Plate Proportional Weir with rectangular, triangular and circular base weir. In the case of the triangular base weir, the asymptotic value of λ (=0.62) compares favourably with the theoretical value of λ(=3/5)(Fig.10(a)). For the rectangular base weir, λ varies slightly above 0.33 when a/R is below 0.35, and it remains nearly constant when a/R exceeds 0.35 and compares well with the theoretical value λ(= 1/3). But, in the circular base weir, the value of λ varies hyperbolically from 0.6 to 0.1 corresponding to the limited range of R_0/R which varies from 2 to 5. It is evident that the more the ratio R_0/R increases the more the datum tends to reach the crest level in order to approach the ideal profile of infinite width. (Fig.10(b) and Fig. 10(c)).

It was noted that the profiles of the exact weirs were generated earlier by complex mathematical formulae and the profiles of the quadrant proportional weirs were generated by using simple expressions. It is interesting to note that the two solutions do not appear to differ very much [2] when selected weirs were chosen for comparison (Fig. 11). Fig. 12 relates the theoretical full discharge Q_0 with the weir dimensions (a/R, b/R, R_0/R) and the maximum deviation(%) from the linearity of Head-Discharge.

These designs have been prepared for a quick solution for a given set of parameters that characterise the weirs flow.

A simple example to illustrate the use of the design chart is provided below.

Requirements: To design a quadrant plate proportional weir with a triangular base weir to carry the full discharge Q_0 = 100 cfs, with R = 3 ft.

$$Q_{non} = \frac{Q_0}{2\ C_d (2g)^{1/2}\ R^{5/2}}$$

$$= \frac{100}{2(.62)[2(32.2)]^{1/2}(3)^{5/2}}$$

$$= 0.64$$

From Fig. 12:

Maximum deviation = 1.1%

a/R = 0.34

b/R = 0.65

Therefore

a = 1.02 ft

b = 1.95 ft

CHAPTER 5

CONCLUSIONS

CHAPTER V

CONCLUSIONS AND SCOPE FOR FURTHER WORK

5.1 CONCLUSIONS

The following conclusions can be drawn on the basis of the present study.

For quadrant plate weirs, the triangular, circular and rectangular shapes can be adopted as suitable base weir profiles. Simple expressions can be developed to relate the geometric variables (ex: R/a, b/a, etc.) of the weirs that ensure linear head discharge relationships.

The data obtained during the experimental program validates the theoretical predictions.

Simple charts have been developed to aid the designers in selecting appropriate basic weir shapes for a required set of weir flow characteristics.

5.2 SCOPE FOR FURTHER WORK

The present study is an extension of the previous work [2] related to linear proportional weirs which have rectangular profiles for base weirs. However, one may change the design approach slightly and examine the effect of replacing the base weir by a simple orifice. Even with a simple rectangular orifice (Fig. 13), one can vary several variables

(Ex: W/R, t/R, S/R) to ensure the desired linear head-discharge relationship for the weir over a wider range of discharges as one has additional variables to select for a given set of flow conditions.

Reference [2a] includes some details of the results of the present study related to linear weirs.

REFERENCES

REFERENCES

[1] Keshavamurthy, K., and Seshagiri, N., "Generalized Mathematical Theory and Experimental Verification of Proportional Notches," Journal of Franklin Institute, Philadelphia, Pa., U.S.A., Vol. 285, No. 5, May 1968, pp.347-363.

[2] Ramamurthy, A.S., Subramanya, K., and Pani, B.S., "The Quadrant Plate Weir," J.Hyd.Div. ASCE, Vol.104, No. 12, Dec. 1977, pp.1431-1441.

[2a] Ramamurthy, A.S. and Pani, B.S., "Solution for Linear Proportional Weir", J. Wastes and Water Eng., Vol.16, No. 1, Jan. 79, pp.50-53.

[3] Rao, Nagar S. Lakshmana, "Theory of Weirs," Advances in Hydroscience, Academic Press Inc., New York, Vol.10, 1975, pp.309-406.

[4] Rao, Nagar S. Lakshmana and Cherengai H. Abdul Bhukari, "Linear Proportional Weir With Trapezoidal Bottoms,"

[5] Venkataraman, P., and Subramanya, K., "A Practical Proportional Weir", Water Power, Vol.25, No.5, May 1973, pp.189-190.

APPENDIX "A"

EXPERIMENTAL DATA

TABLE A.1

EXPERIMENTAL DATA FOR SERIE 1

Q → cfs

H → in

V → fps

R = 5"

a = 2.50"

b = 4.16"

Total number of experiments = 56

1	2	3	4	5	6	7	8
Q_{ac}	H	Q_{ac}/Q_0	H/R	Q_{non}	C_d	V	Fr
			P = 9.50"				
.902	7.50	1.000	1.500	.833	.603	.477	.071
.810	6.90	.898	1.380	.750	.601	.444	.067
.771	6.64	.855	1.328	.715	.600	.429	.065
.744	6.46	.825	1.292	.690	.600	.419	.064
.702	6.21	.778	1.242	.653	.598	.402	.062
.640	5.77	.709	1.154	.593	.600	.377	.059
.538	5.13	.596	1.026	.500	.599	.330	.052
.443	4.47	.491	.894	.410	.602	.285	.047
.349	3.89	.387	.778	.325	.598	.234	.039
.262	3.30	.290	.660	.243	.600	.184	.031
.182	2.76	.201	.552	.170	.598	.133	.023

(continued)

1	2	3	4	5	6	7	8
Q_{ac}	H	Q_{ac}/Q_0	H/R	Q_{non}	C_d	V	Fr
			P = 5"				
.893	7.35	.976	1.470	.814	.610	.650	.113
.871	7.24	.952	1.448	.798	.606	.640	.112
.794	6.70	.868	1.340	.722	.612	.610	.109
.707	6.19	.773	1.238	.648	.607	.568	.104
.640	5.70	.699	1.140	.580	.614	.538	.100
.547	5.09	.598	1.018	.496	.614	.487	.094
.444	4.41	.485	.882	.402	.615	.424	.084
.350	3.81	.382	.762	.320	.609	.357	.073
.247	3.18	.270	.636	.226	.608	.271	.058
.152	2.56	.181	.513	.140	.604	.180	.040
			P = 2.37"				
.922	7.47	.997	1.494	.830	.618	.843	.164
.891	7.27	.963	1.454	.803	.617	.831	.163
.808	6.76	.873	1.352	.733	.613	.796	.161
.737	6.30	.797	1.260	.666	.616	.765	.159
.673	5.92	.727	1.184	.612	.613	.730	.155
.621	5.51	.671	1.102	.555	.623	.709	.154
.536	4.96	.579	.992	.480	.621	.658	.148
.446	4.38	.482	.876	.396	.627	.594	.139
.359	3.84	.388	.768	.320	.625	.520	.127
.260	3.21	.281	.642	.232	.623	.419	.108
.167	2.63	.180	.526	.150	.619	.300	.082

(continued)

1	2	3	4	5	6	7	8
Q_{ac}	H	Q_{ac}/Q_0	H/R	Q_{non}	C_d	V	Fr
			P = 1.11"				
.937	7.49	.997	1.498	.833	.626	.980	.204
.899	7.23	.956	1.446	.795	.629	.970	.205
.824	6.76	.876	1.352	.730	.628	.942	.205
.758	6.31	.806	1.262	.670	.630	.919	.206
.692	5.93	.736	1.186	.612	.630	.884	.203
.628	5.48	.668	1.096	.550	.636	.857	.204
.550	4.94	.585	.988	.480	.638	.818	.203
.458	4.39	.487	.878	.397	.642	.749	.195
.366	3.83	.389	.766	.316	.644	.666	.183
.268	3.23	.285	.646	.232	.643	.555	.162
.180	2.69	.191	.538	.157	.638	.426	.133
			P = 0.24"				
.952	7.36	.981	1.472	.815	.650	1.127	.250
.928	7.21	.957	1.442	.796	.649	1.121	.251
.902	7.05	.930	1.410	.772	.650	1.113	.252
.857	6.79	.883	1.358	.732	.651	1.097	.253
.800	6.40	.825	1.280	.680	.655	1.084	.257
.727	5.93	.749	1.186	.612	.660	1.060	.261
.658	5.47	.678	1.094	.550	.666	1.037	.265
.600	5.11	.618	1.022	.500	.668	1.009	.266
.530	4.67	.546	.934	.440	.671	.971	.267
.444	4.15	.458	.830	.365	.676	.910	.265

(continued)

1	2	3	4	5	6	7	8
Q_{ac}	H	Q_{ac}/Q_0	H/R	Q_{non}	C_d	V	Fr
			P = 0.24"				
.353	3.64	.364	.728	.292	.673	.818	.253
.260	3.11	.268	.622	.216	.670	.698	.233
.167	2.54	.172	.508	.140	.666	.540	.198

TABLE A.2

EXPERIMENTAL DATA FOR SERIE 2

Q → cfs

H → in

V → fps

R = 5.25"

a = 1.84"

b = 3.42"

Total number of experiments = 43

1	2	3	4	5	6	7	8
Q_{ac}	H	Q_{ac}/Q_0	H/R	Q_{non}	C_d	V	Fr
			P = 9.50"				
.792	7.01	1.000	1.350	.650	.599	.432	.065
.768	6.84	.972	1.303	.623	.606	.432	.065
.702	6.40	.889	1.219	.575	.600	.397	.061
.614	5.74	.777	1.093	.500	.604	.363	.057
.526	5.04	.666	.960	.425	.609	.326	.052
.457	4.55	.578	.867	.373	.603	.293	.048
.316	3.48	.400	.663	.253	.614	.219	.037
.171	2.42	.216	.461	.137	.614	.129	.023

(continued)

1	2	3	4	5	6	7	8
Q_{ac}	H	Q_{ac}/Q_0	H/R	Q_{non}	C_d	V	Fr
			P = 5"				
.727	6.50	.901	1.238	.585	.611	.569	.102
.652	5.90	.808	1.124	.523	.613	.538	.100
.559	5.21	.693	.992	.445	.618	.493	.094
.465	4.49	.576	.855	.365	.627	.441	.087
.378	3.82	.464	.728	.295	.630	.386	.079
.267	3.04	.331	.579	.204	.644	.299	.064
.169	2.38	.209	.453	.130	.640	.206	.046
			P = 2.50"				
.773	6.81	.948	1.297	.620	.613	.747	.150
.740	6.55	.908	1.247	.592	.611	.736	.149
.687	6.14	.843	1.169	.546	.619	.716	.149
.623	5.67	.764	1.080	.495	.619	.686	.147
.578	5.33	.709	1.015	.456	.624	.664	.145
.498	4.72	.611	.899	.390	.628	.621	.141
.419	4.14	.514	.788	.325	.634	.568	.135
.347	3.58	.426	.682	.265	.644	.514	.127
.265	2.99"	.325	.569	.200	.652	.434	.113
.172	2.33	.211	.444	.130	.651	.320	.090

(continued)

1	2	3	4	5	6	7	8
Q_{ac}	H'	Q_{ac}/Q_0	H/R	Q_{non}	C_d	V	Fr
			P = 1.12"				
.823	7.10	1.000	1.352	.650	.623	.901	.192
.752	6.56	.914	1.249	.594	.623	.881	.194
.685	6.05	.832	1.152	.536	.628	.860	.196
.624	5.59	.758	1.065	.486	.632	.837	.197
.540	4.97	.656	.947	.420	.633	.798	.197
.440	4.27	.535	.813	.340	.637	.735	.193
.361	3.67	.439	.699	.274	.648	.678	.189
.266	2.97	.323	.566	.200	.654	.585	.177
.174	2.35	.211	.447	.130	.659	.451	.148
			P = 0.18"				
.823	6.96	.976	1.326	.635	.638	1.037	.237
.737	6.31	.874	1.202	.565	.642	1.022	.246
.677	5.85	.803	1.114	.515	.647	1.010	.251
.619	5.40	.734	1.028	.465	.655	.998	.267
.534	4.78	.633	.910	.396	.656	.969	.266
.440	4.11	.522	.783	.323	.665	.923	.272
.350	3.49	.415	.665	.255	.675	.858	.274
.263	2.89	.312	.550	.187	.678	.771	.269
.174	2.29	.206	.436	.123	.682	.634	.246

TABLE A.3

EXPERIMENTAL DATA FOR SERIE 3

Q → cfs R = 5"

H → in a = 1.87"

V → fps b = 4.52"

Total number of experiments = 58 R_0 = 15"

1	2	3	4	5	6	7	8
Q_{ac}	H	Q_{ac}/Q_0	H/R	Q_{non}	C_d	V	Fr
P = 9.50"							
.916	6.77	.980	1.354	.860	.593	.507	.077
.851	6.33	.910	1.266	.795	.596	.484	.074
.760	5.76	.813	1.152	.710	.596	.448	.070
.697	5.36	.745	1.072	.650	.597	.422	.067
.635	4.95	.679	.990	.590	.599	.395	.063
.549	4.41	.587	.882	.510	.599	.355	.058
.457	3.81	.489	.762	.420	.605	.309	.052
.365	3.27	.390	.654	.340	.597	.257	.044
.262	2.63	.280	.526	.240	.607	.194	.034
.163	2.01	.174	.402	.150	.605	.127	.023

(continued)

1	2	3	4	5	6	7	8
Q_{ac}	H	Q_{ac}/Q_0	H/R	Q_{non}	C_d	V	Fr
			P = 5"				
.955	6.76	.971	1.352	.860	.618	.731	.130
.846	6.09	.861	1.218	.760	.619	.686	.126
.789	5.71	.803	1.142	.705	.623	.663	.124
.700	5.15	.712	1.030	.620	.628	.621	.119
.652	4.82	.663	.964	.570	.636	.598	.117
.564	4.33	.574	.866	.495	.634	.544	.109
.461	3.73	.469	.746	.403	.637	.475	.098
.370	3.17	.376	.634	.325	.633	.408	.087
.256	2.50	.260	.500	.223	.639	.307	.068
.155	1.93	.158	.386	.135	.639	.201	.047
			P = 2.60"				
.961	6.68	.963	1.336	.845	.633	.932	.187
.946	6.59	.948	1.318	.833	.632	.926	.186
.902	6.33	.904	1.266	.795	.631	.909	.186
.846	5.99	.848	1.198	.740	.636	.886	.185
.815	5.75	.817	1.150	.710	.639	.878	.185
.752	5.39	.753	1.078	.655	.639	.847	.183
.695	5.05	.696	1.010	.603	.641	.818	.181
.585	4.37	.586	.874	.504	.646	.755	.175
.514	3.94	.515	.788	.440	.650	.707	.169
.433	3.50	.449	.700	.370	.651	.639	.158

(continued)

1	2	3	4	5	6	7	8
Q_{ac}	H	Q_{ac}/Q_0	H/R	Q_{non}	C_d	V	Fr
			P = 2.60"				
.348	3.00	.345	.600	.296	.654	.559	.144
.254	2.45	.254	.490	.215	.657	.452	.112
.172	1.97	.172	.394	.145	.660	.339	.097

(continued)

1	2	3	4	5	6	7	8
Q_{ac}	H	Q_{ac}/Q_0	H/R	Q_{non}	C_d	V	Fr
			P = 1.15"				
.982	6.63	.948	1.326	.840	.650	1.136	.249
.961	6.47	.928	1.294	.816	.655	1.135	.251
.928	6.27	.896	1.254	.790	.654	1.126	.252
.882	6.02	.851	1.204	.750	.654	1.107	.252
.846	5.78	.817	1.156	.710	.663	1.099	.255
.786	5.45	.759	1.090	.666	.657	1.072	.255
.727	5.08	.702	1.016	.605	.669	1.050	.257
.661	4.70	.638	.940	.550	.669	1.017	.257
.615	4.40	.594	.880	.505	.677	.997	.258
.530	3.90	.511	.780	.430	.686	.945	.257
.444	3.40	.434	.680	.360	.686	.878	.251
.358	2.93	.341	.586	.290	.687	.790	.234
.260	2.41	.251	.482	.210	.689	.657	.212
.174	1.92	.168	.384	.140	.691	.510	.178
			P = 0.38"				
.979	6.42	.923	1.284	.806	.676	1.296	.303
.940	6.20	.887	1.240	.775	.675	1.286	.306
.896	5.96	.845	1.192	.740	.674	1.272	.308
.859	5.75	.810	1.150	.708	.675	1.261	.311
.750	5.12	.707	1.024	.613	.681	1.227	.320
.642	4.45	.606	.890	.513	.696	1.196	.332
.568	4.05	.536	.810	.450	.702	1.154	.335

(continued)

1	2	3	4	5	6	7	8
Q_{ac}	H	Q_{ac}/Q_0	H/R	Q_{non}	C_d	V	Fr
			P = 0.38"				
.502	3.64	.474	.728	.395	.707	1.124	.342
.405	3.13	.382	.626	.316	.713	1.038	.338
.328	2.72	.309	.544	.255	.716	.952	.330
.246	2.26	.232	.452	.190	.720	.839	.315

DRAWINGS

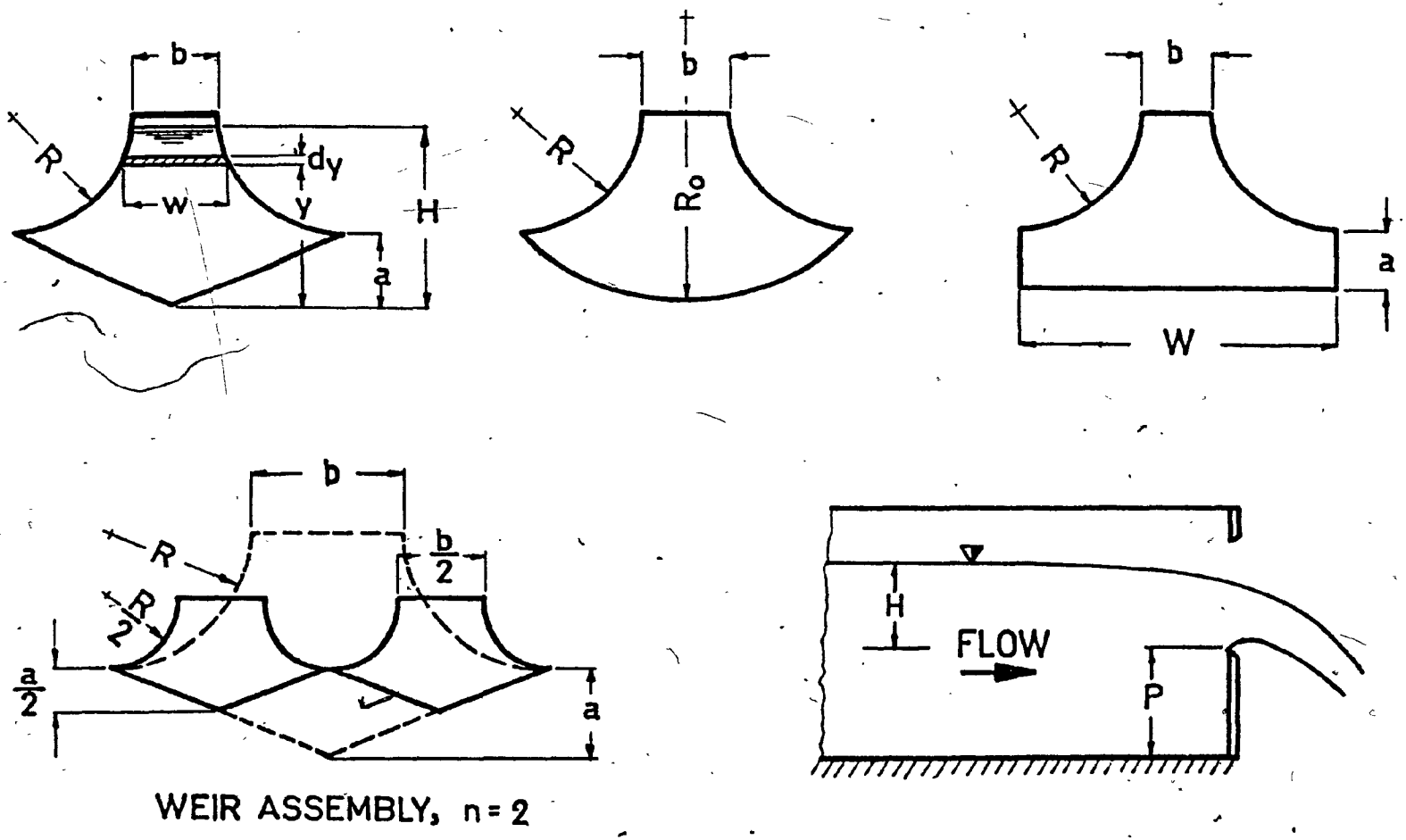

WEIR ASSEMBLY, n = 2

FIG. 1 WEIR NOTATIONS

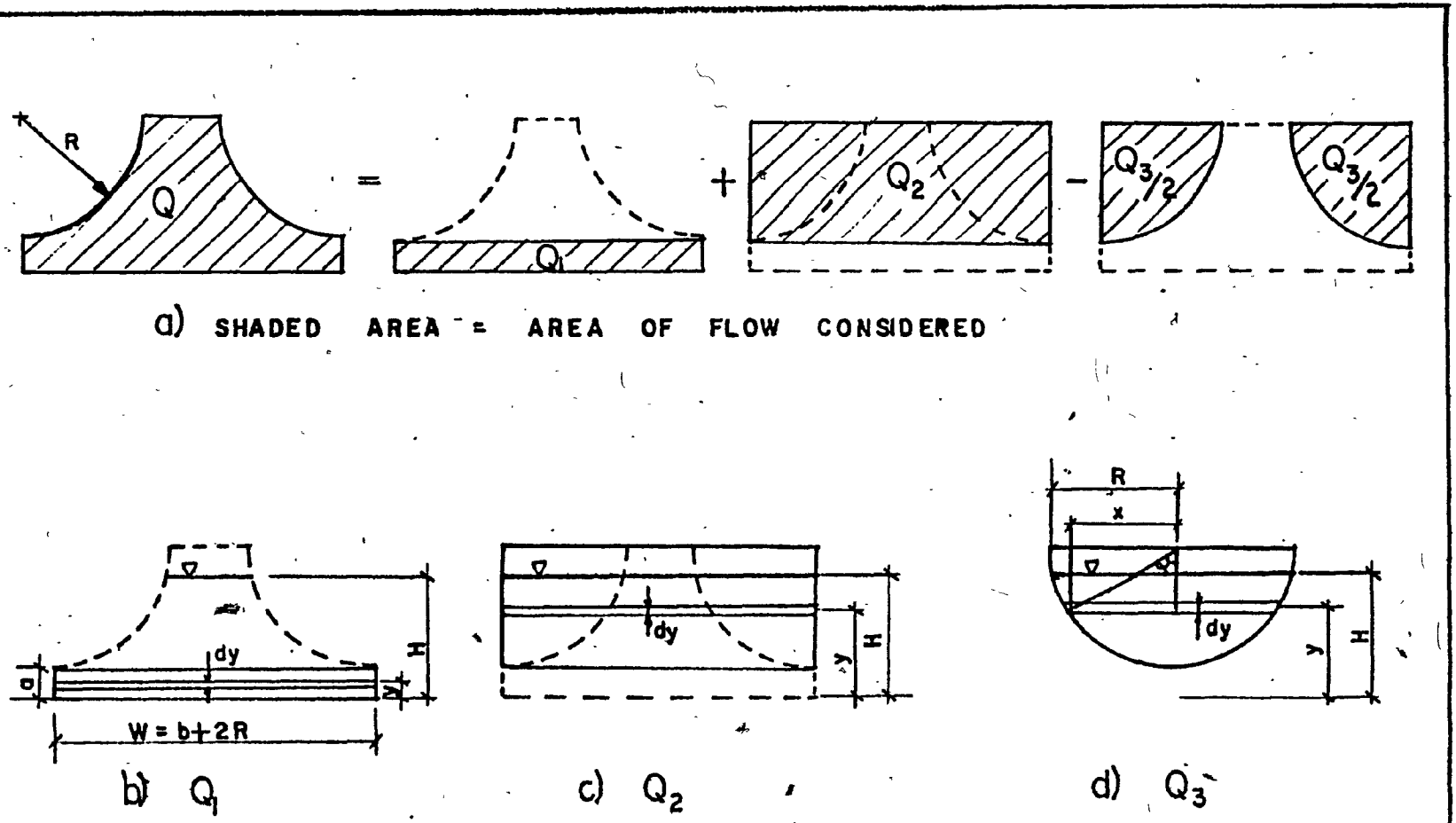

FIG. 2 SCHEME FOR INTEGRATION OF WEIR DISCHARGE WITH RECTANGULAR BASE WEIR

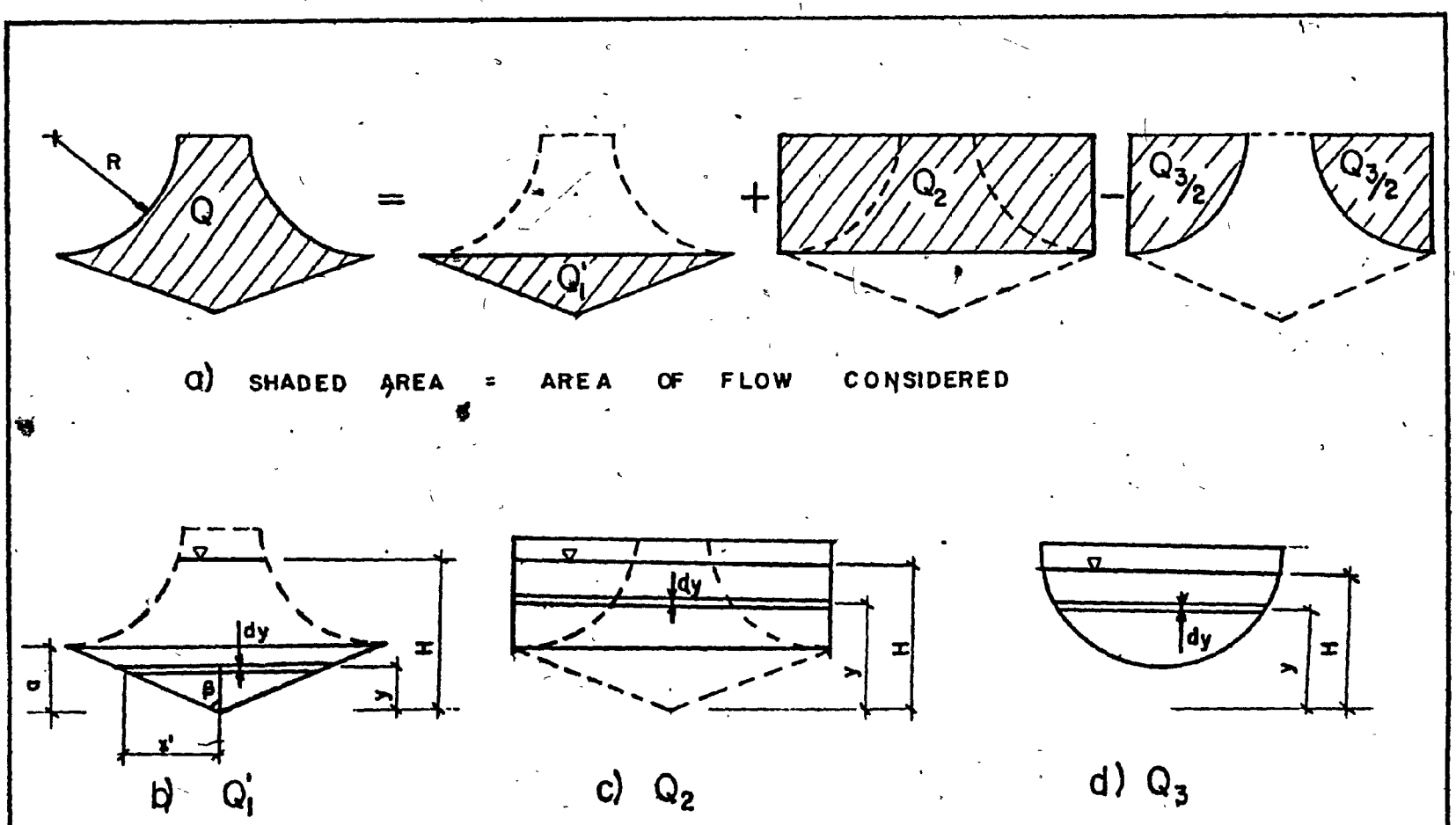

FIG. 3 SCHEME FOR INTEGRATION OF WEIR DISCHARGE WITH TRIANGULAR BASE WEIR

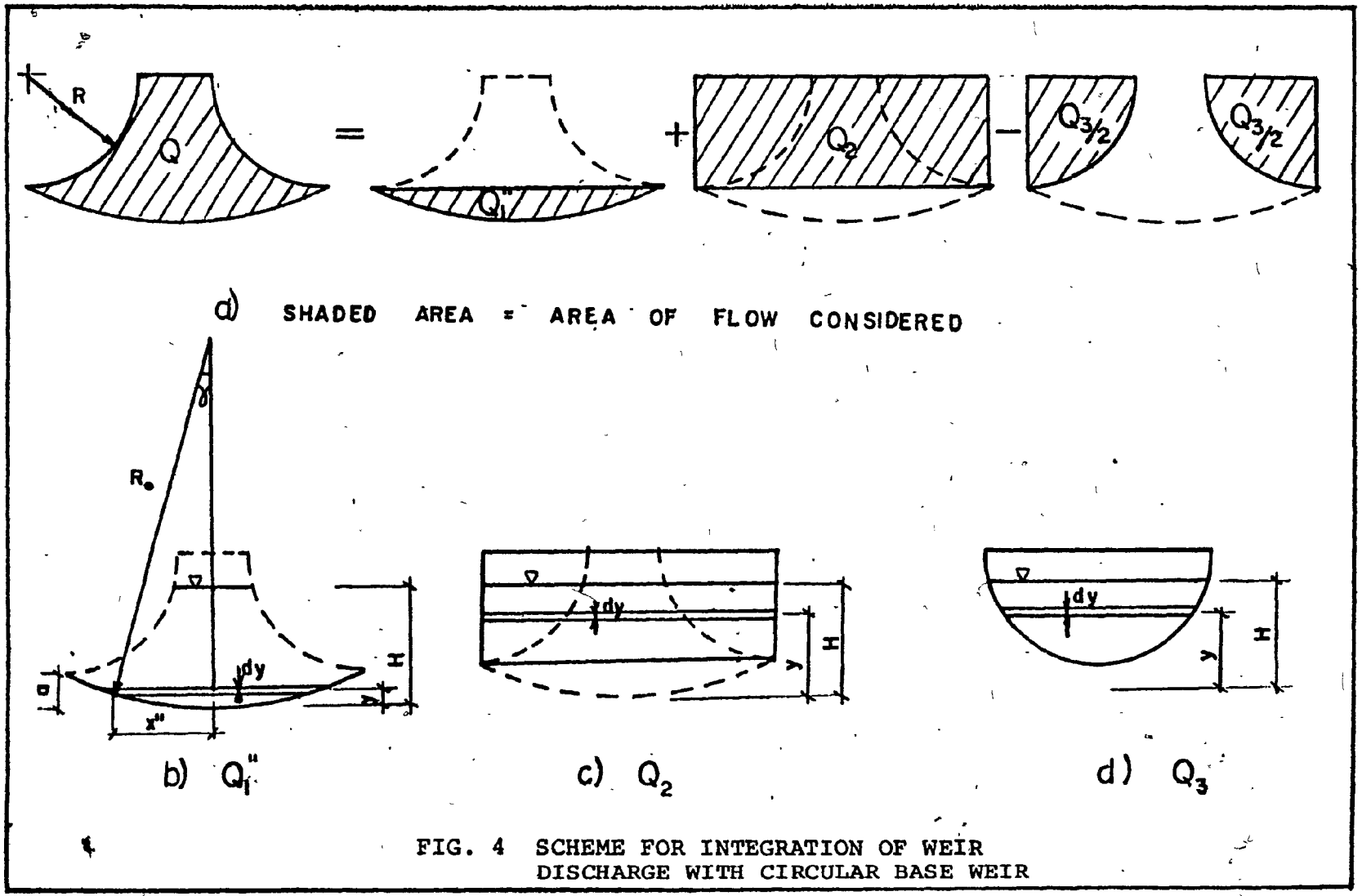

FIG. 4 SCHEME FOR INTEGRATION OF WEIR DISCHARGE WITH CIRCULAR BASE WEIR

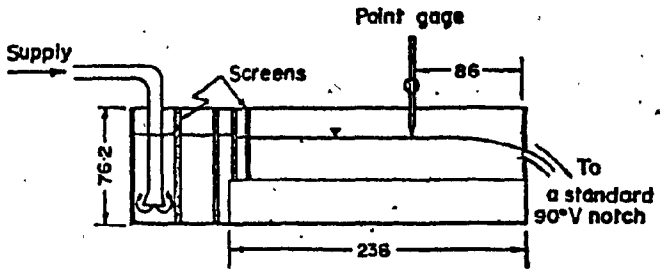

(a) ELEVATION

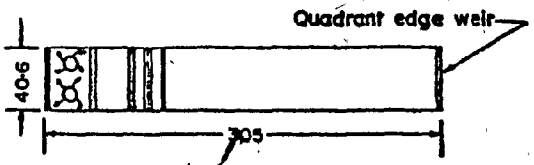

(b) PLAN

All dimensions are in centimeters

FIG. 5 EXPERIMENTAL LAYOUT

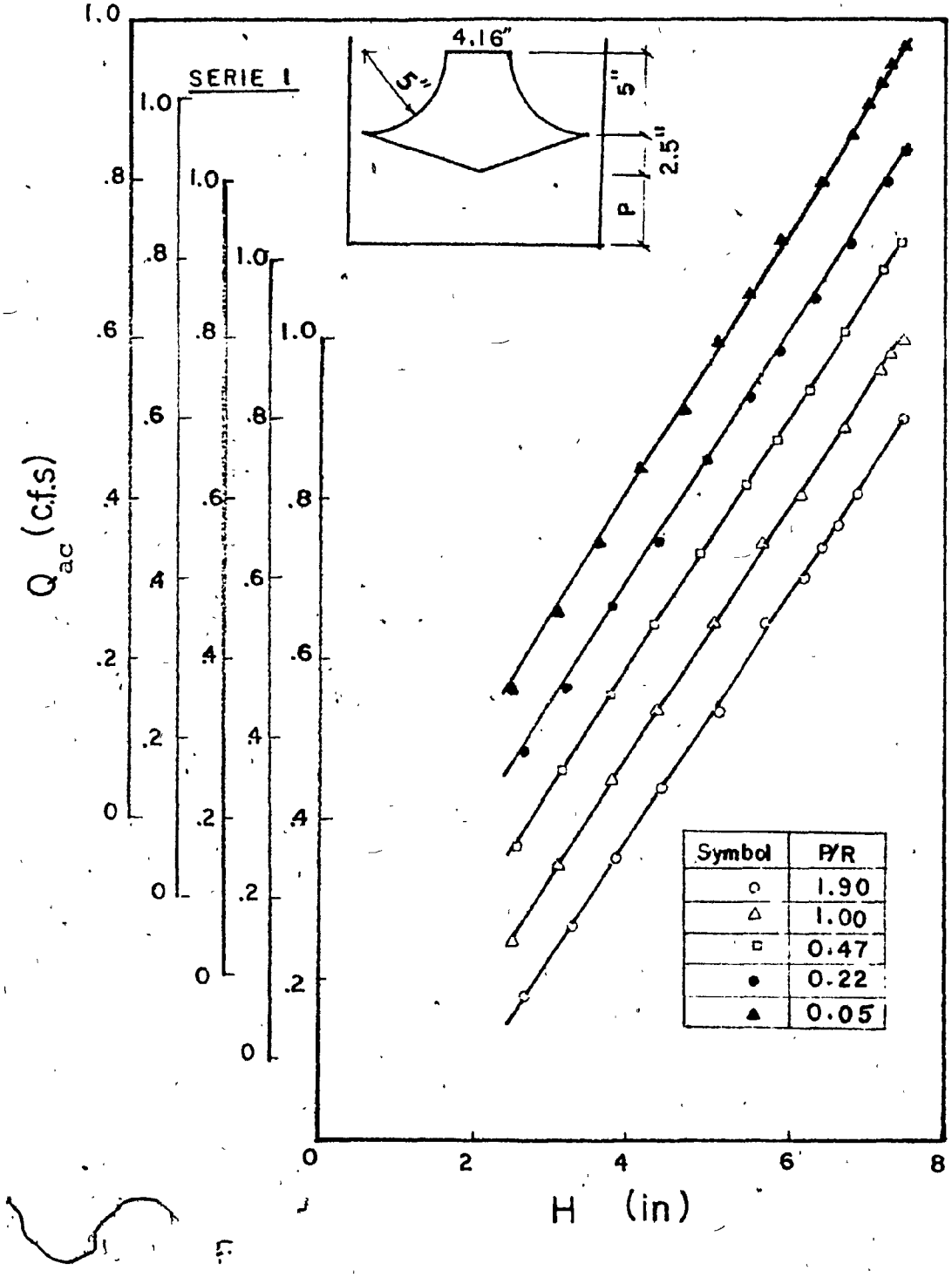

FIG. 6 RATING CURVE: HEAT H VERSUS ACTUAL DISCHARGE Q_{ac}

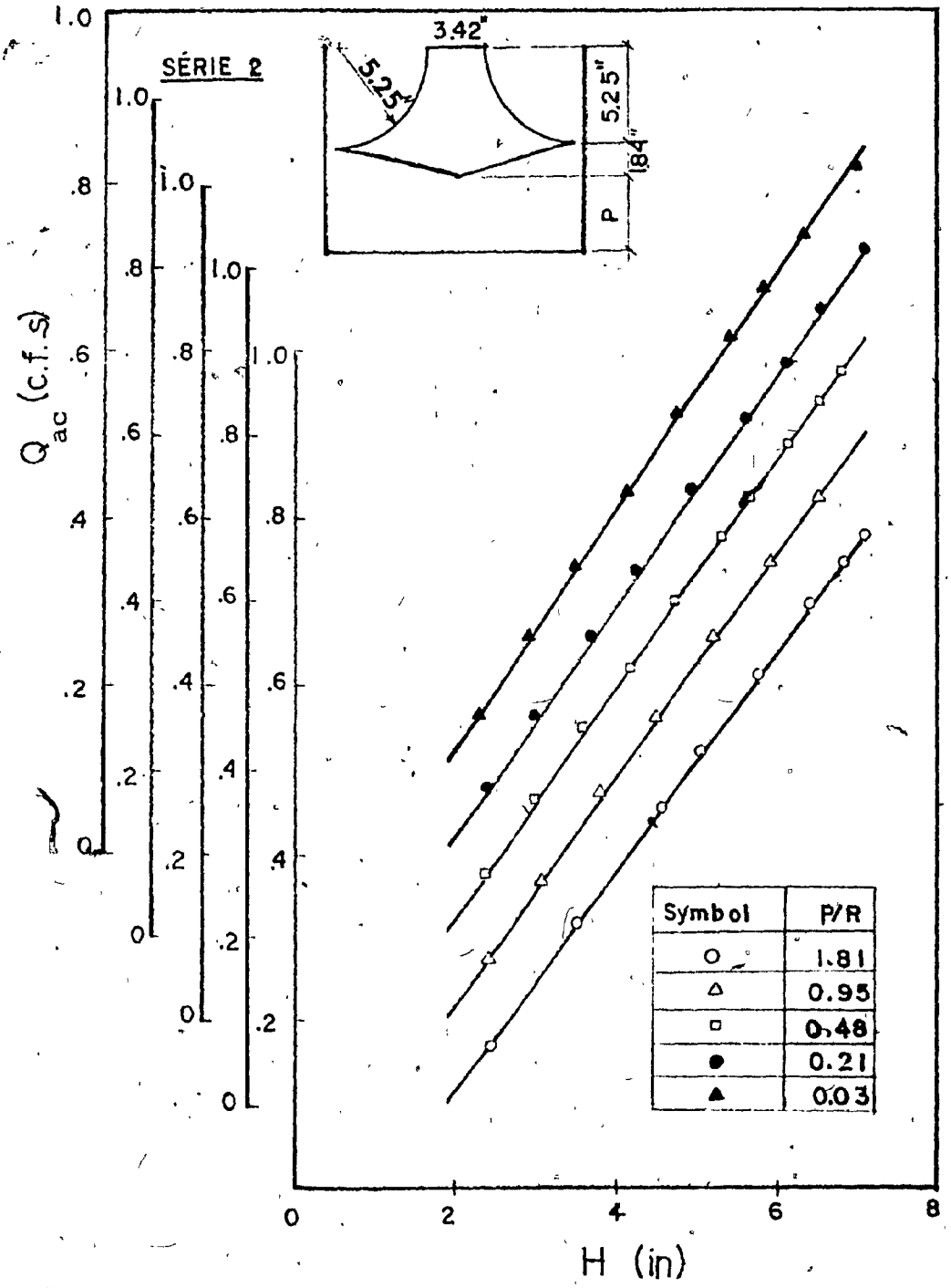

FIG. 6 (continued)

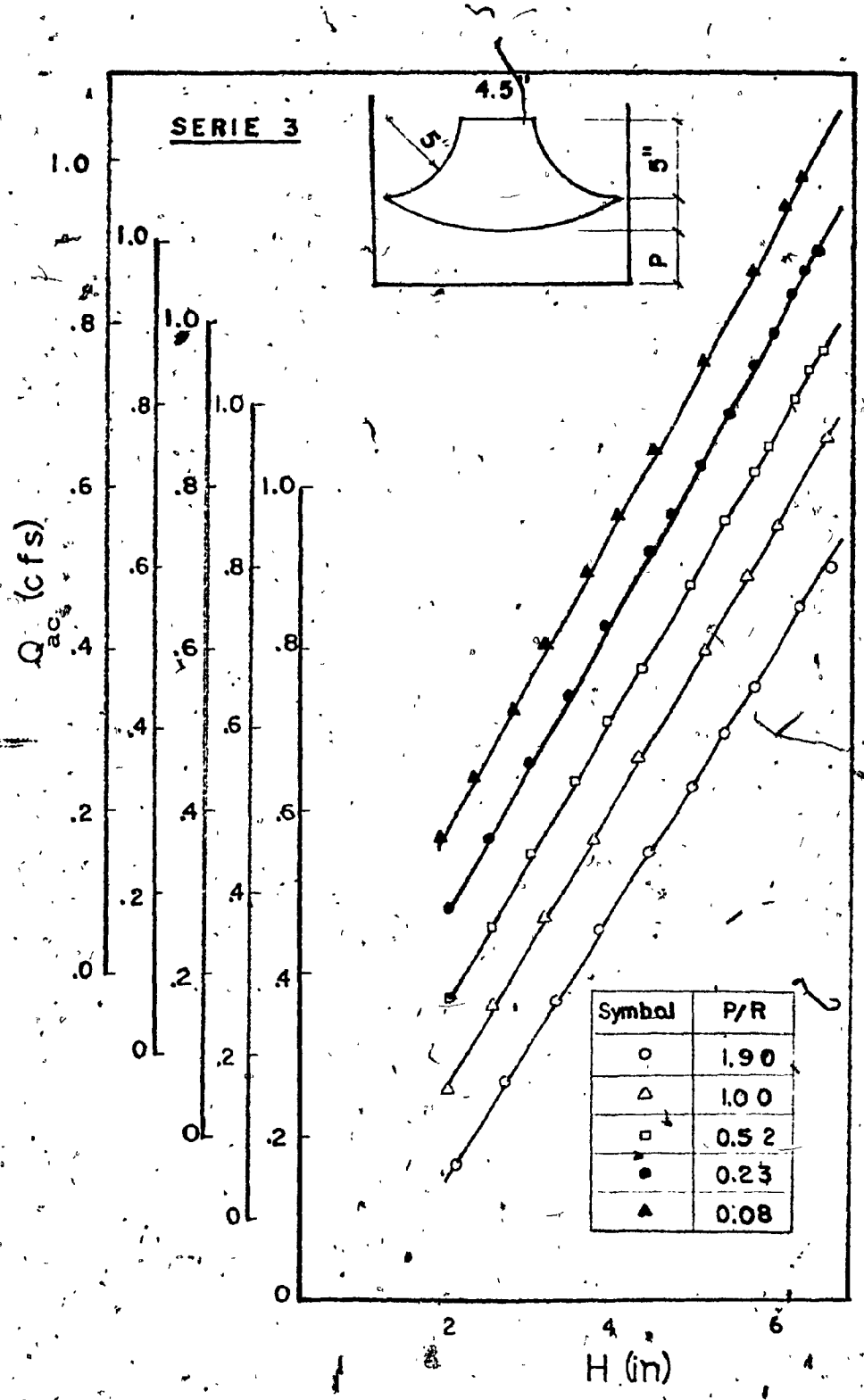

FIG. 6 (continued)

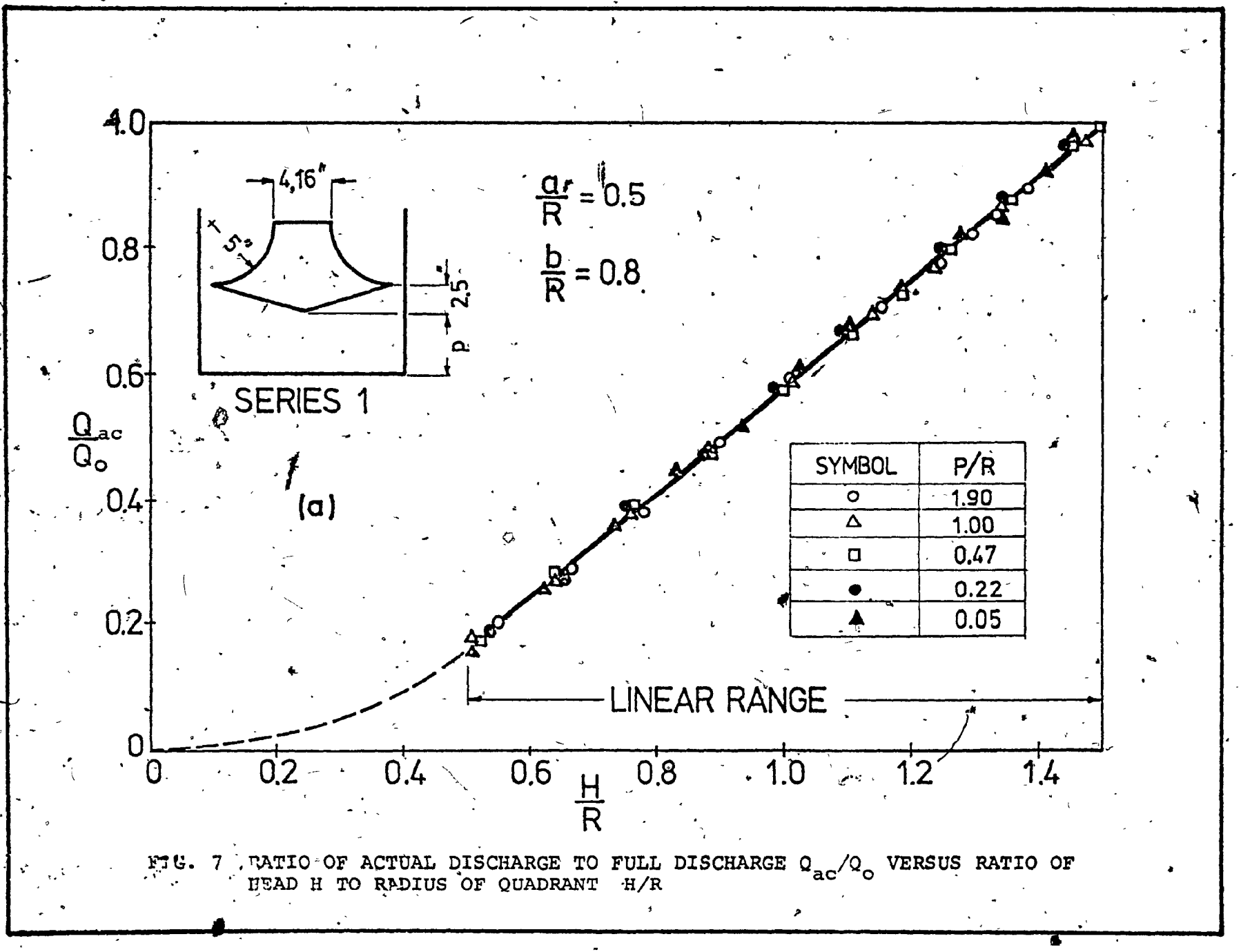

FIG. 7 RATIO OF ACTUAL DISCHARGE TO FULL DISCHARGE Q_{ac}/Q_o VERSUS RATIO OF HEAD H TO RADIUS OF QUADRANT H/R

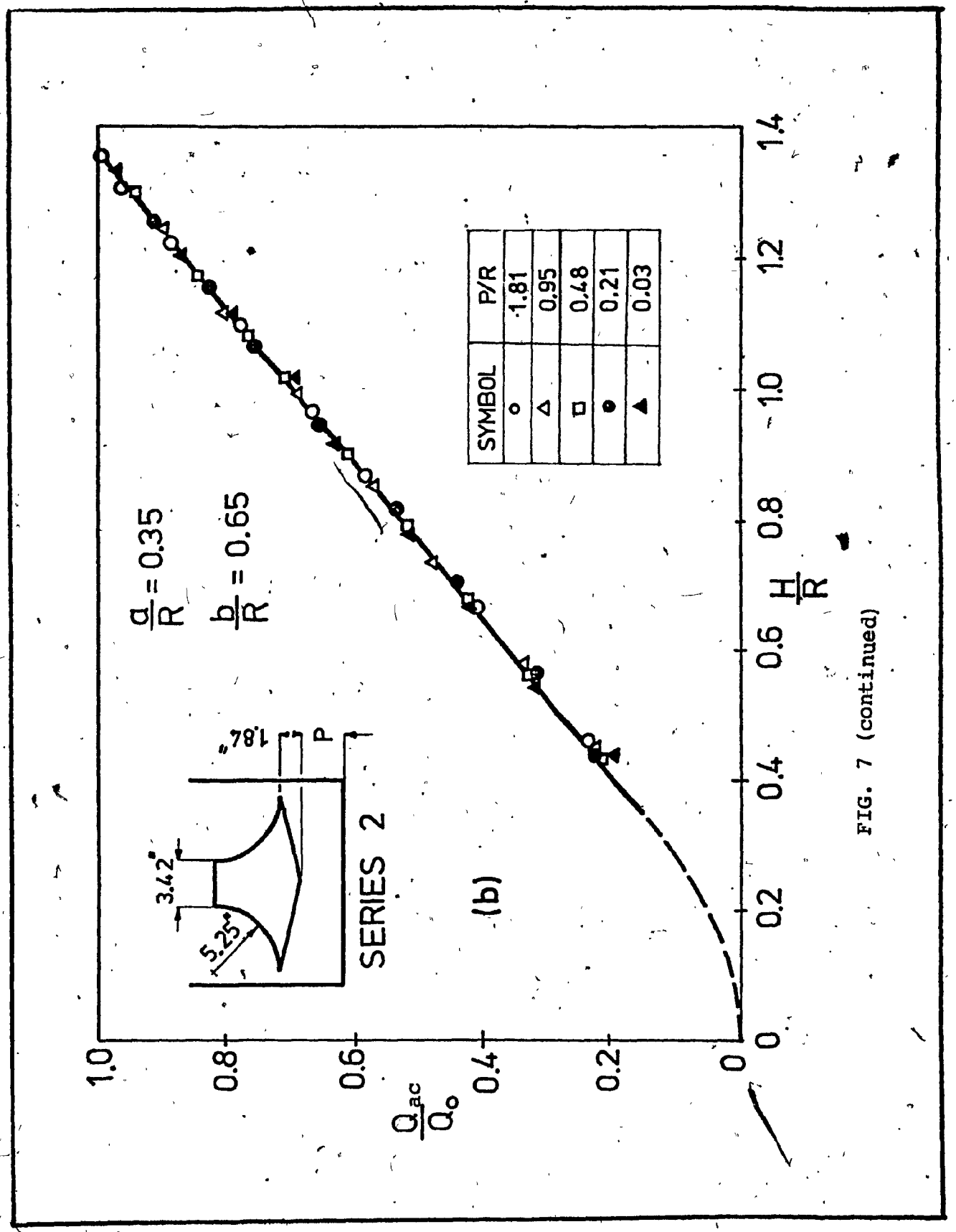

FIG. 7 (continued)

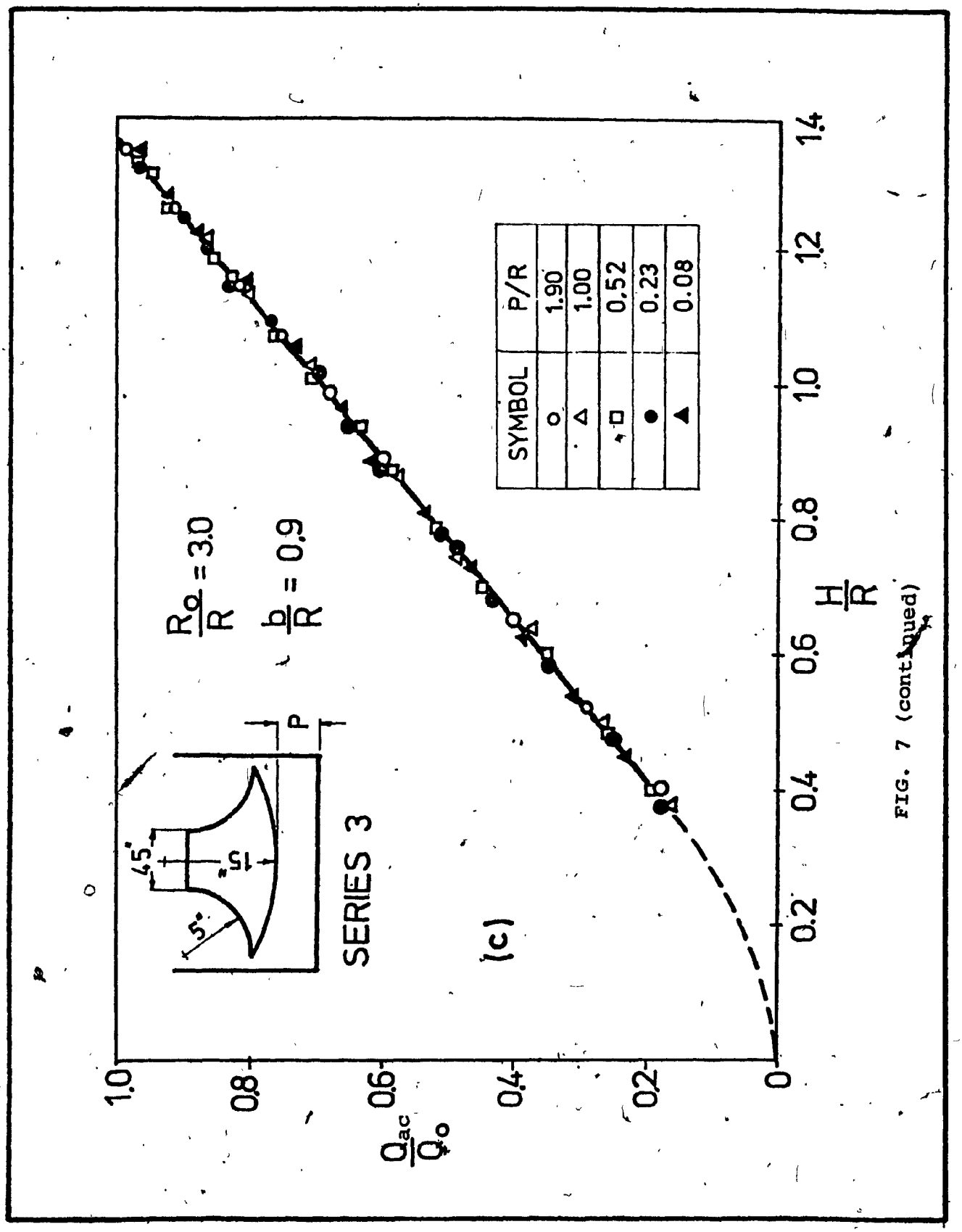

FIG. 7 (continued)

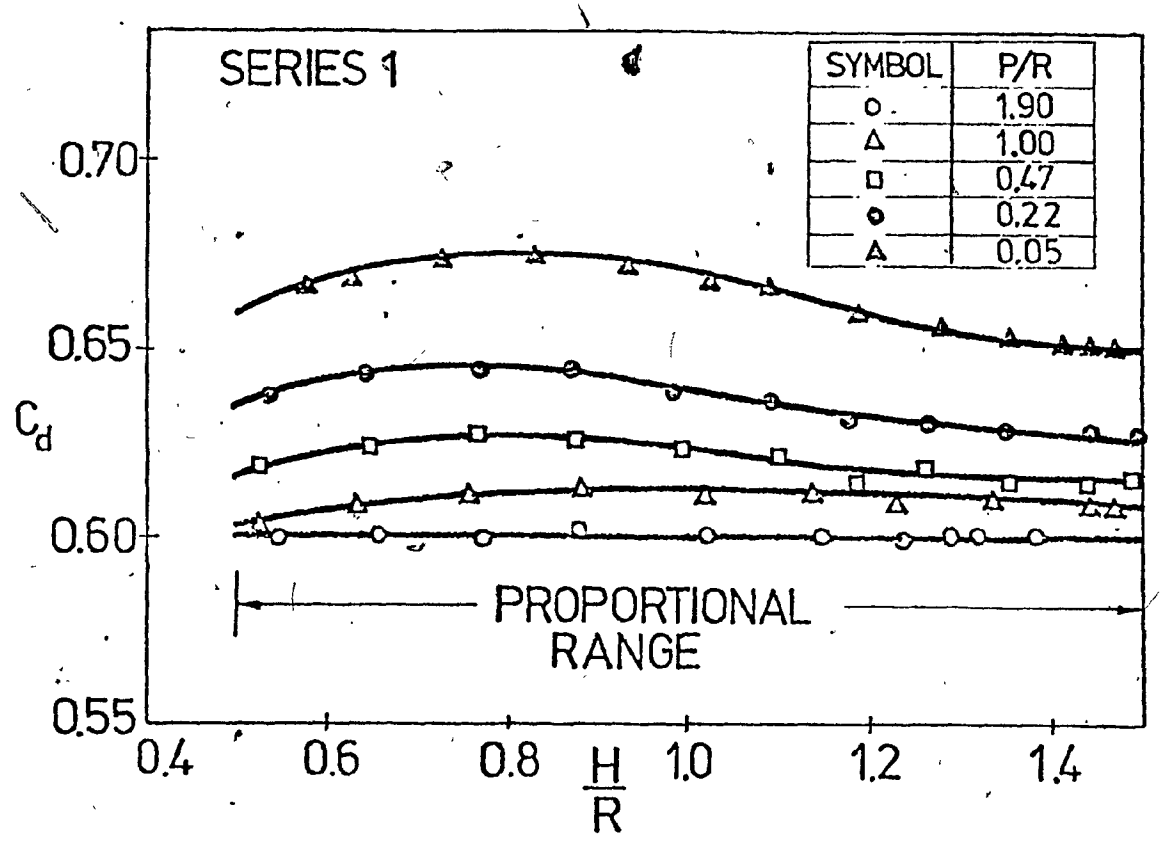

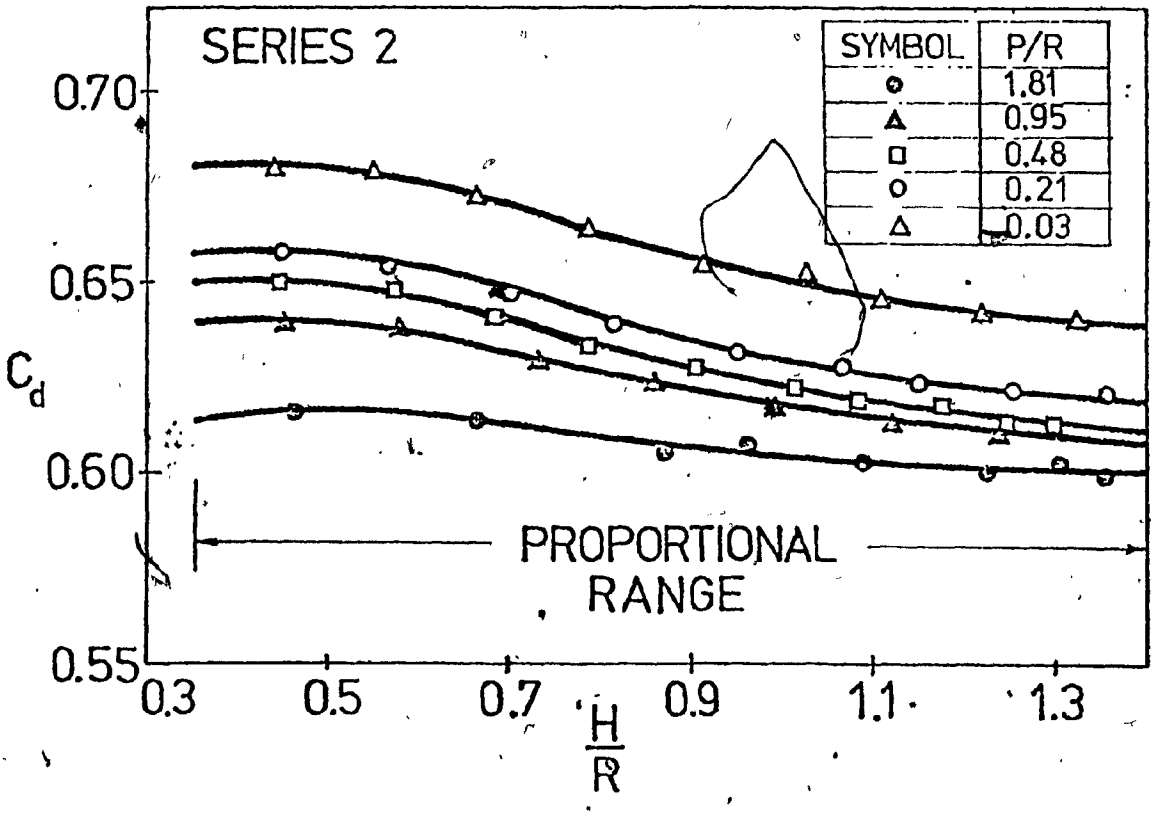

FIG. 8 VARIATION OF COEFFICIENT OF DISCHARGE C_d VERSUS RATIO OF HEAD TO RADIUS OF QUADRANT H/R

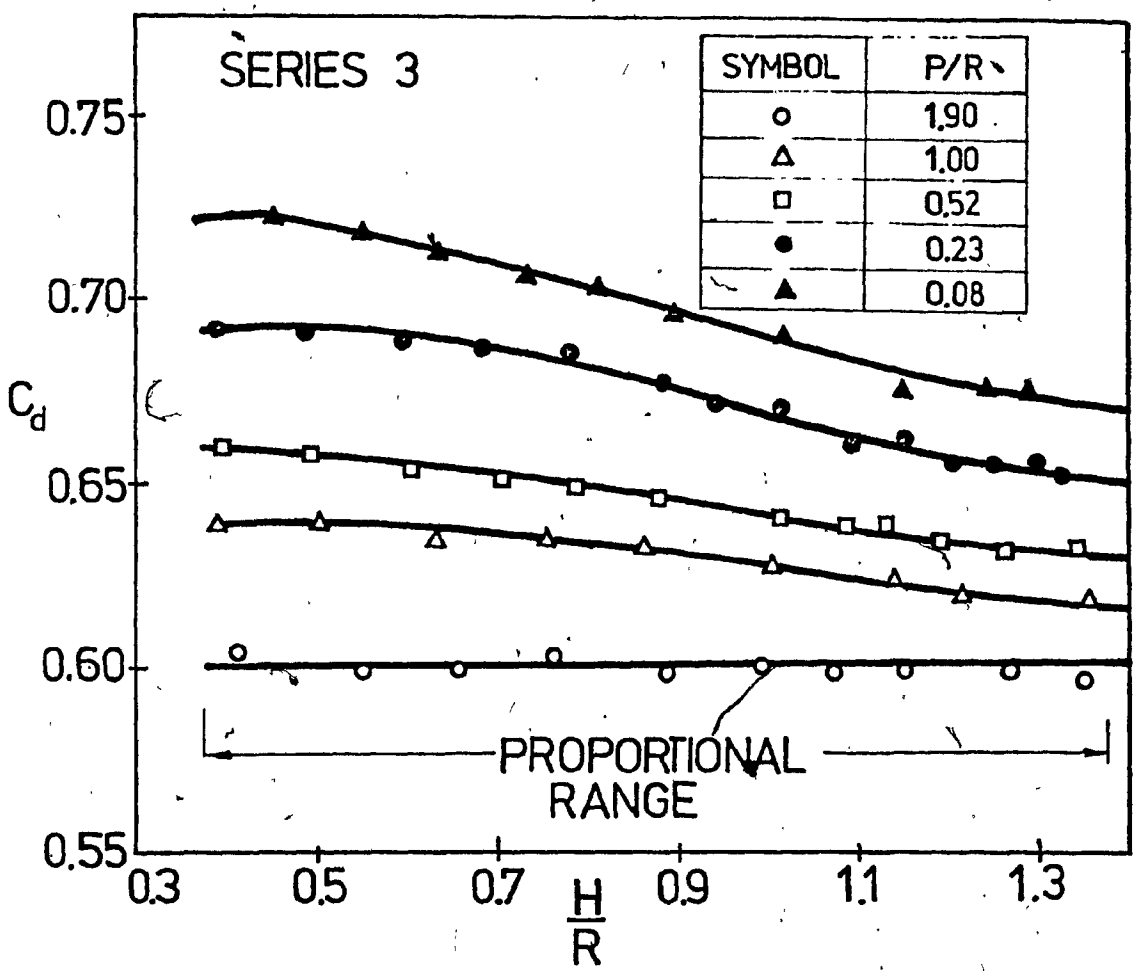

FIG. 8 (continued)

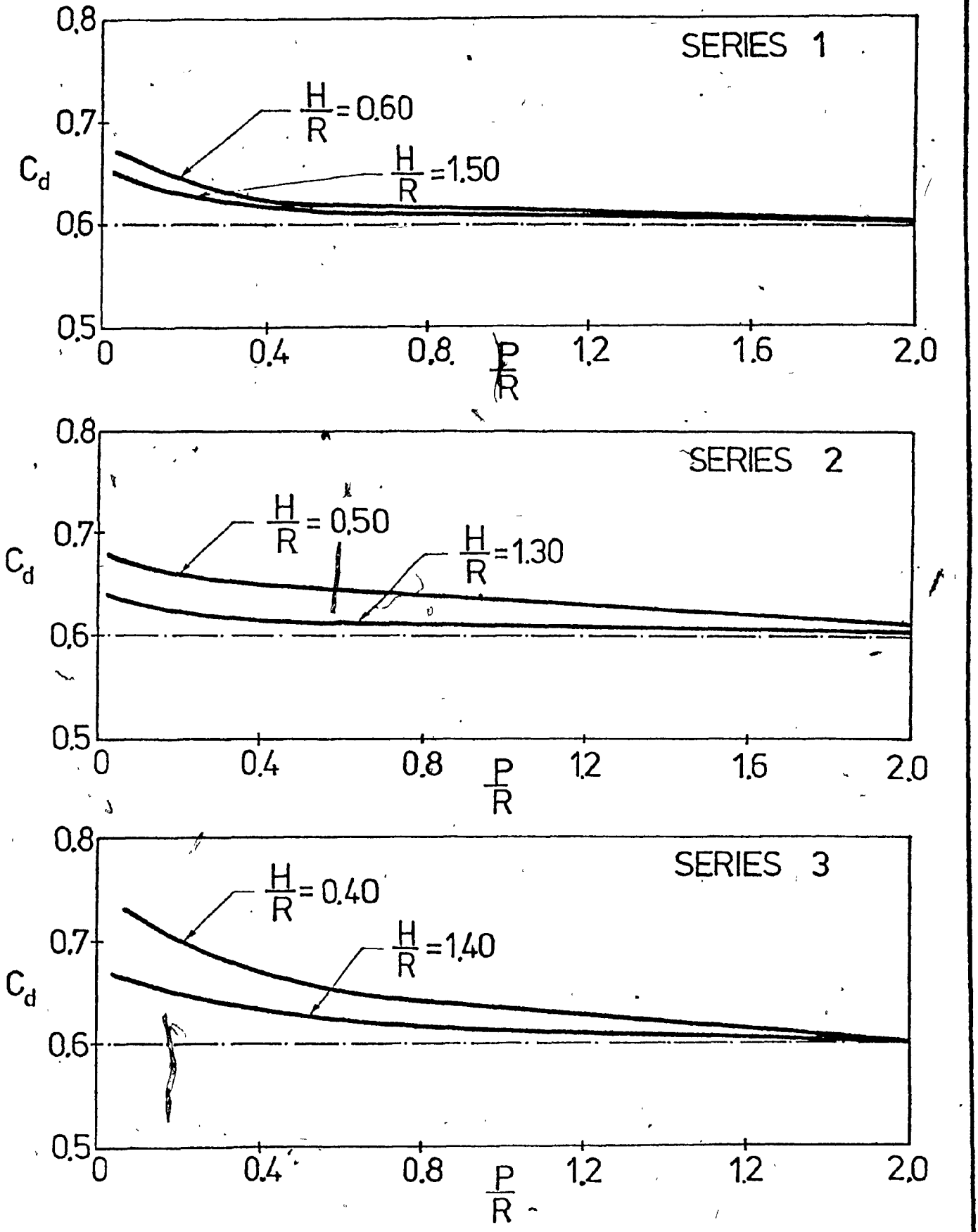

FIG. 9 VARIATION OF COEFFICIENT OF DISCHARGE C_d VERSUS RATIO OF HEIGHT OF THE CREST TO RADIUS OF QUADRANT P/R

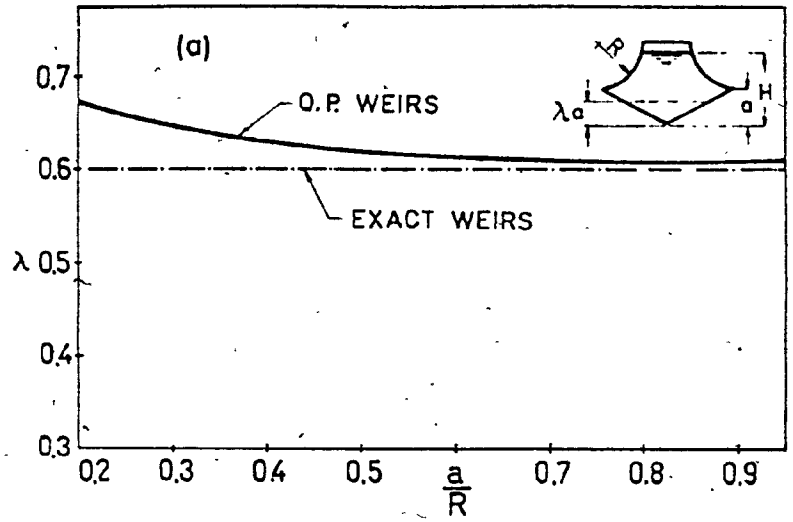

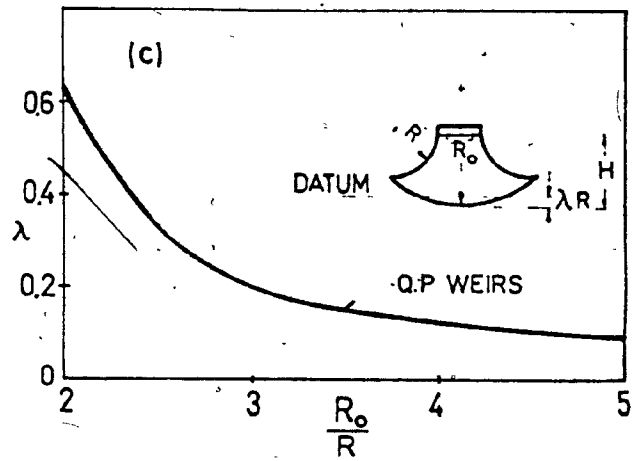

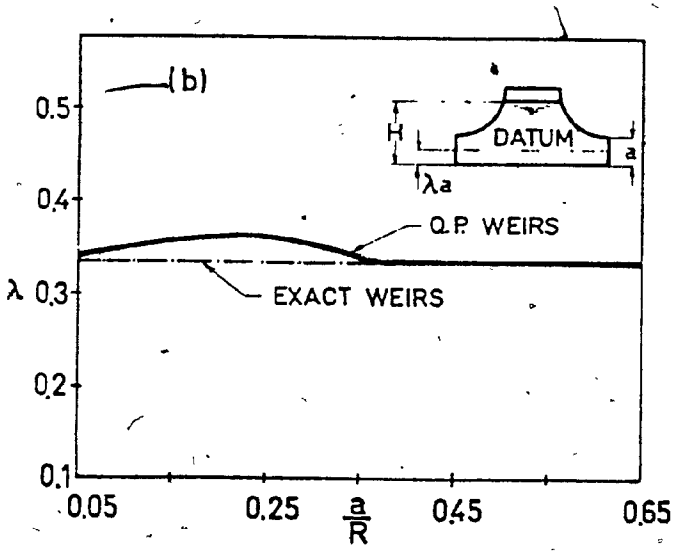

CASE (a) & (b) $Q = K(H - \lambda a)$

CASE (c) $Q = K(H - \lambda R)$

FIG. 10 VARIATION OF FACTOR OF REDUCTION OF HEAD λ VERSUS RATIO OF HEIGHT OF WEIR BASE a OR RADIUS OF CIRCULAR WEIR BASE R_o TO RADIUS OF QUADRANT R, a/R OR R_o/R

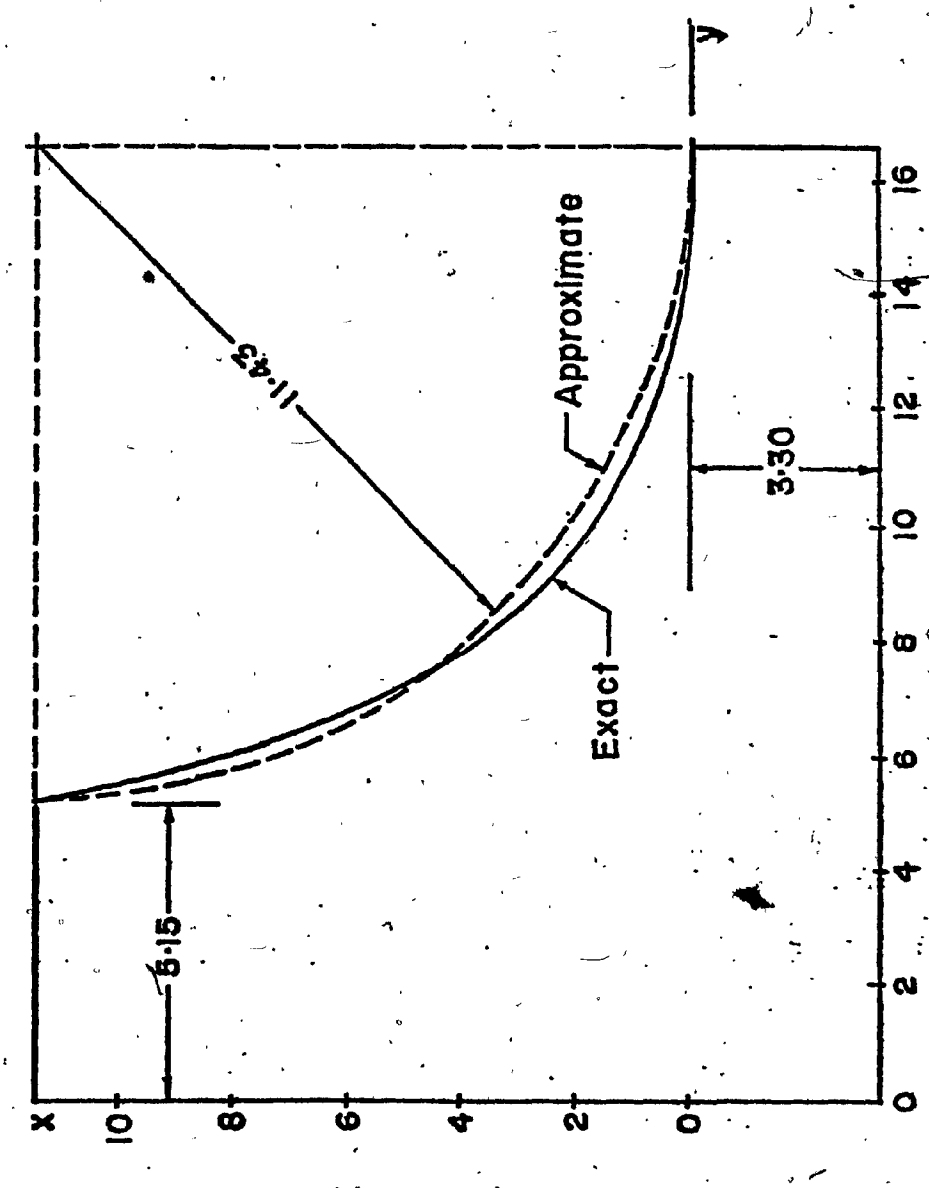

FIG. 11 GRAPHICAL FIT

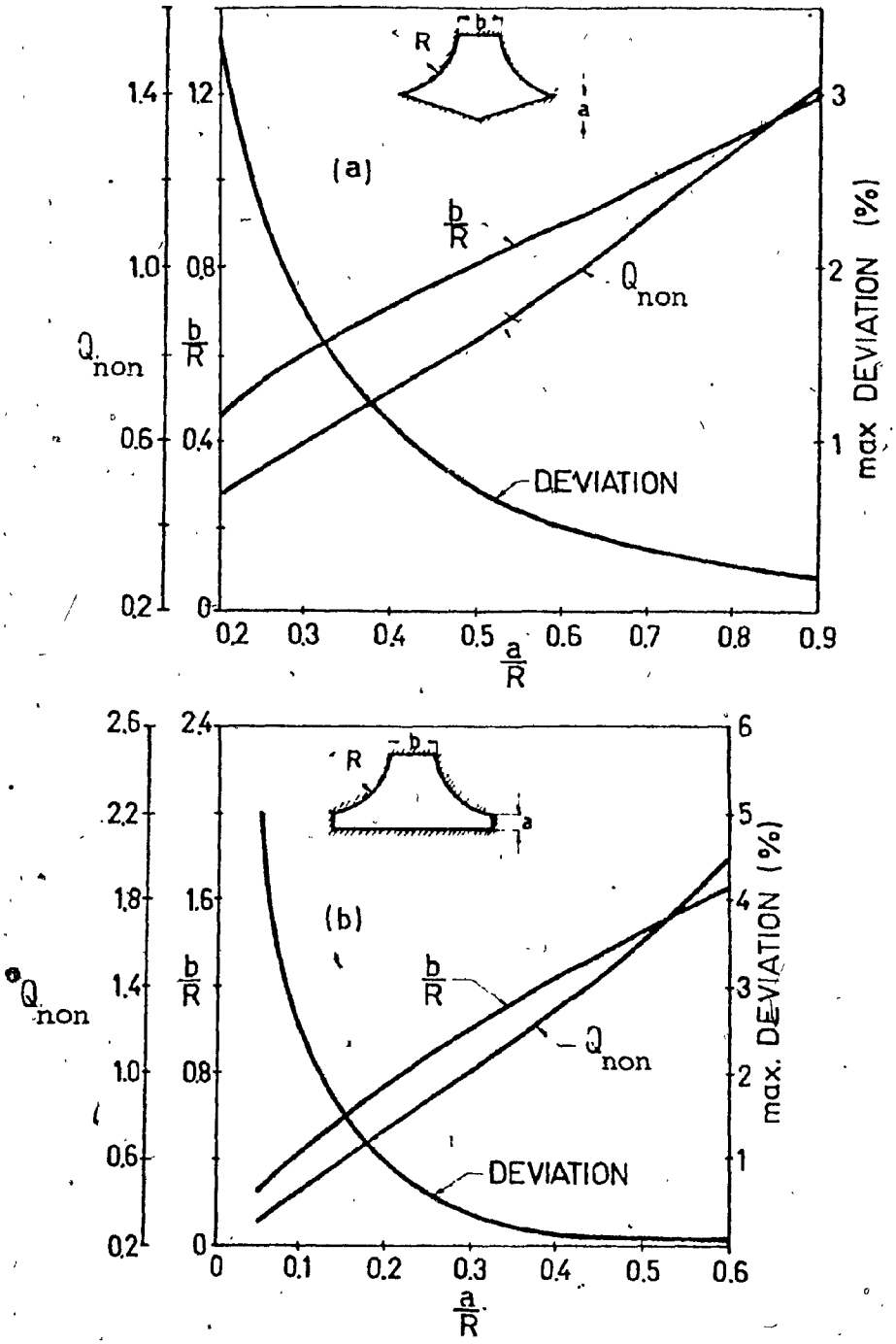

FIG. 12 DESIGN CHARTS

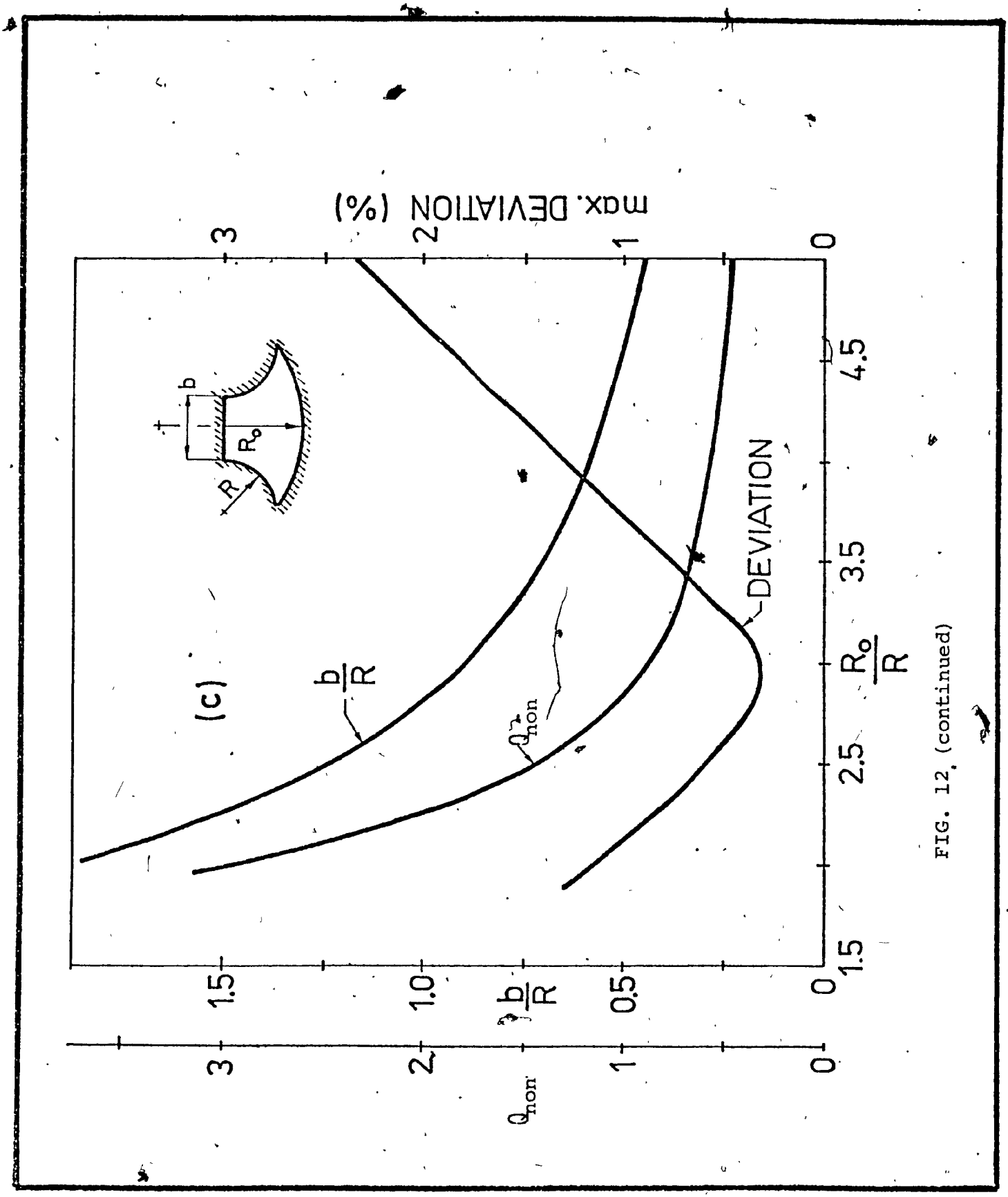

FIG. 12 (continued)